Mass and isospin breaking effects in the Skyrme model and in holographic QCD

Lorenzo Bartolini,[1] Stefano Bolognesi,[2] Sven Bjarke Gudnason,[1,*] and Tommaso Rainaldi[3]

[1]*Institute of Contemporary Mathematics, School of Mathematics and Statistics, Henan University, Kaifeng, Henan 475004, People's Republic of China*

[2]*Department of Physics "E. Fermi," University of Pisa and INFN Sezione di Pisa Largo Pontecorvo, 3, Edificio C, 56127 Pisa, Italy*

[3]*Department of Physics, Old Dominion University, Norfolk, Virginia 23529, USA*

(Received 23 April 2024; accepted 11 June 2024; published 17 July 2024)

We discuss how the quark masses and their mass splitting affect the baryons in the Skyrme model as well as the Witten-Sakai-Sugimoto (WSS) model. In both cases, baryons are described by solitonic objects, i.e., Skyrmions and instantons, respectively. After the quantization of their zero modes, the nucleons become quantum states of a rotor. We show how the quark mass affects the moment of inertia and we provide a semianalytic approach valid in the small-mass limit. Additionally, we show how the two lightest quarks' mass splitting affects the moments of inertia of the Skyrmion and induces an isospin breaking effect. This effect turns out not to be enough to split the degeneracy in the neutron-proton multiplet, but it splits some of the states in the Δ multiplet. Unlike the basic Skyrme model, the WSS model already includes vector mesons and another mechanism to transfer isospin breaking from quark masses to the solitons is known. We compute the splitting of the moment of inertia in the small-mass limit in the WSS model and combine the two effects on the spectrum of baryons, in particular the Δ's.

DOI: 10.1103/PhysRevD.110.026017

I. INTRODUCTION

The Skyrme model [1,2] provides us with a tool to probe low-energy QCD and understand baryon phenomenology, see the reviews [3,4]. Results can be obtained from a pure mesonic pseudoscalar theory and baryons are solitonic objects in this theory. The skyrmion configuration then needs to be quantized to obtain the full spectrum of possible baryons: This can be done in the moduli space quantization scheme [5]. However, there is a missing piece of the bigger picture. One problem, in particular, which is left unresolved in the pseudoscalar theory alone, is the isospin breaking effect and how it is transmitted from the quarks to the nucleons.

It is well known in the literature that the addition of the quark mass in the Skyrme model induces a pion mass in the low-energy effective theory [6]. This has already been extensively studied within the Skyrme model [7–11]. The first part of this paper is devoted to the case of equal quark masses and how this affects the moment of inertia of the skyrmion. We show that there is a way to treat the problem semianalytically in the limit of small mass, using the linear tail of the pions, where the pion mass is induced by the quark mass. In this regime the main correction to the moment of inertia is linear in the pion mass m. A nontrivial aspect of this computation is that the first-order approximation has a divergence, which eventually is resolved by the nonlinear core of the skyrmion, but we are able to prove that this term contributes only at order m^2 and thus can be neglected at the linear order in m. This contribution depends only on the coefficient in front of the linear tail, which can be computed at $m = 0$ and is related to the $g_{NN\pi}$ coupling. For the Skyrme model, we also perform the full computation numerically; we have done it for the spherical case (quarks with equal masses) and confirmed the validity of the above semianalytic approximation. The physical intuition of why the dominant effect on the moment of inertia from turning on a small pion mass comes from the tail of the soliton is this. The small pion mass changes the solution only very little in energy and hence the core of the solution is almost unchanged. On the other hand, the tail of the soliton goes from a power law at zero mass to an exponential falloff at a finite pion mass, and hence the tail is the most sensitive to a tiny pion mass. The total mass of the soliton changes only very little, but the moment of inertia is

*Contact author: gudnason@henu.edu.cn

roughly weighted with r^2 compared with the energy density and hence is very sensitive to any change in the tail.

Splitting in baryonic masses is hard to obtain by first-principles computations. The full theory of QCD should be tackled with nonperturbative techniques, so the only viable options up to now have been lattice formulation and chiral effective theories, like the Skyrme model. In this work, we will introduce isospin breaking in the quark mass matrix and examine how this affects the skyrmion (baryon) configuration from the point of view of its symmetry properties, moduli space, and quantum states.

Adding an isospin breaking term to the effective Lagrangian is not difficult, and we want to do it in the most simple and natural way; that is, by introducing a splitting in the pion mass term. We know that this is the right way to do it, as in the standard model the isospin breaking is transferred from the Yukawa couplings to the quark mass term and then to the pion mass term through the Gell-Mann-Oakes-Renner relation. The first problem we encounter is that, in the $SU(2)$ model alone, this term has no physical effect on the pions. To make the effect visible, we have to extend the theory to $U(2)$ and thus consider also the η meson. We then have a measurable isospin splitting in the pion mass matrix. But this is not the end of the story; the difficult part then is to transfer this isospin breaking to the skyrmion sector. If we consider just the $SU(2)$ pions and the quark mass splitting, we do not see any effect at all, not even in the pion spectrum. In order to see a splitting in the pion masses and consequently a deformation of the skyrmion, we need to introduce at least the η field, the pseudo-Nambu-Goldstone boson of the axial $U(1)_A$ anomalous symmetry. With this minimally extended model, we can have isospin breaking in the pion masses and consequently a splitting in the moments of inertia of the skyrmion.

The mass splitting of the pions affects the skyrmion already at the classical level, once we relax the assumption of the hedgehog approximation. The skyrmion remains axially symmetric, but becomes prolate or oblate (this has to be determined and may be not obvious *a priori*). We devised a semianalytic method to compute the deformation of the inertia tensor in the small-mass limit. We then tested this in the Skyrme model where the full numerical computations can be made. Still the quantization of the skyrmion moduli space does not provide a mass splitting between neutron and proton states. It provides a partial splitting in the Δ particles' masses.

It has been argued [3,12–17] that an extension of the Skyrme model with vector mesons can answer many of the unsolved questions left from the pseudoscalar theory. Any precise model describing nucleon interactions should also take into account heavier particles, such as the lightest vector mesons, whose masses are around 780 MeV; the presence of these new particles certainly has an impact on the structure and the spectrum of the skyrmion, see, e.g., Refs. [18,19]. Another reason, comes from the validity of the large-N_c theory that views baryons as solitons of an effective theory of both pseudoscalars and vector mesons that are actually predicted by the large-N_c theory [20].

The early literature on the proton-neutron mass splitting in the Skyrme model context started with computations of a current-current electromagnetic contribution to the splitting [21]—a formula derived in the bag model of quarks using the one-particle exchange Feynman diagram [22]. Their result was both incorrect in sign and numerically inaccurate, as pointed out shortly after in Ref. [23]. The intuition from the bag model was that the quark mass splitting in the bag model would give rise to a too large positive mass splitting between the neutron and the proton of about 1.79 MeV, whereas the subdominant negative current-current electromagnetic contribution would be around −0.50 MeV, lowering the result of the mass splitting to roughly the correct experimental value [23]. As was also pointed out in Ref. [23], the $SU(2)$ Skyrme model with isospin breaking in terms of a nonderivative potential is not able to provide the contribution to the neutron-proton mass splitting. Soon after a new mechanism for introducing a nonelectromagnetic neutron-proton mass splitting in the Skyrme model was proposed in Ref. [24], where experimental evidence of nonelectromagnetic isospin breaking in $\rho-\omega$ meson mixing led the authors to introduce a term $\lambda\rho_\mu\omega^\mu$ into the Skyrme model. The neutron-proton mass splitting was not computed by computing the impact on the skyrmion itself, but rather by performing a current-current computation of the ρ meson and the ω meson, giving a formula of the same kind as the electromagnetic contribution, albeit this time with the necessary positive sign [24]. The only role of the Skyrme model in this computation was to evaluate the strong interaction form factors in this Feynman diagram of a vector boson exchange between nucleons. Using phenomenological input data, this result gave a splitting of the right order of magnitude within the usual 30% accuracy.

A result more in the spirit of using the skyrmion as the nucleon was obtained by Jain *et al.* [25], where the model is extended from $SU(2)$ to $U(2)$, by adding the η meson, and the ρ and ω mesons are added as well. Their paper is concerned with getting the correct strong sector contribution to the neutron-proton mass splitting and involves many explicit chiral symmetry breaking terms of four categories as well as "cranking" corrections, which are essential in their approach. As for the mechanism of the neutron-proton mass splitting, their result was nicely summarized in the review [16], where it was pointed out that the dominant source of the neutron-proton mass splitting comes from the mass term that is directly proportional to the down-up quark mass difference. Although this term sources the η field, the source is

proportional to the quark mass splitting ϵ, making the resulting field η proportional to ϵ and in turn the contribution to the energy proportional to ϵ^2 and both the neutron and the proton would receive the same correction. Their mechanism works by including a source for the η by an approach dubbed a cranking mechanism, which consists of gauging an anomaly term that contains the Wess-Zumino term and three other anomalous pieces [see the term proportional to d_1 of Eq. (3.11) in Ref. [15]]. The coefficient is determined by computing the electromagnetic $\omega \to \gamma\pi^0$ decay rate [13]. The contribution of this "gauging" to the electroweak current acts as a source for the η that is not proportional to the quark mass splitting, but requires the ω vector meson to the present. This turning on of the η field then gives the dominant contribution to the neutron-proton mass splitting from the pion mass term, in the mechanism of Ref. [25].

Results for the neutron-proton mass splitting were also obtained by several groups in chiral bag models, which are conceptually somewhat different from the Skyrme-type models in that they include explicit quark fields that become important in the core of the "skyrmion," e.g., [25,26]. An obvious conceptual challenge with this approach is whether there is any overcounting in the nucleon of the quark degrees of freedom or not, although this has been argued not to be a problem since the quarks are dominantly present in the core of the nucleon and the pion cloud is dominant outside the core. We will not discuss the neutron-proton mass splitting in those models here, but refer to the literature [25,26].

It is worth mentioning that another recent model in the literature [27] achieved the neutron-proton mass splitting in the Skyrme model by adding an isospin breaking term as a derivative coupling between the ω meson and the charged pions. Not including the neutral pion thus explicitly breaks isospin symmetry. Although this mechanism is simple and provides a neutron-proton mass splitting, it is not clear to us whether this term can be derived as an effective Lagrangian term induced from the quark mass difference or whether it can be embedded into a holographic model. We want to pursue the more traditional approach of inducing only the isospin breaking in the mass term, as this is what we expect from chiral effective theory and the standard model.

Our result in Sec. II of this paper is that we can analytically compute the coefficient of the contribution to the moment of inertia which is linear in the pion mass. Since it is quadratic in the mass splitting parameter, it is also quadratic in the isospin quantum number and provides no contribution to the neutron-proton mass splitting, as mentioned above, but it provides a splitting between the masses of the isospin $\frac{3}{2}$ and isospin $\frac{1}{2}$ Δ's.

In order to move toward the more realistic picture of the isospin breaking effects, we thus need to take into account the following:

(i) the η field [corresponding to extending $SU(2)$ to $U(2)$] and
(ii) providing a source of the η that does not originate from the isospin breaking $\pi^0\eta$ vertex (the mass term itself).

Reference [25] used the ω meson and cranking to arrive at a physical neutron-proton mass splitting. We will choose a slightly different route, which we consider to be somewhat easier than introducing the vector mesons in the Skyrme model with the gauged Wess-Zumino-Witten term, other gauged anomalous terms as well as the η field—we will consider the Witten-Sakai-Sugimoto (WSS) model, which contains all the vector mesons, the η as well as the gauged anomalous term as its five-dimensional Chern-Simons term. The advantage here will be that we can utilize the Belavin-Polyakov-Schwartz-Tyupkin (BPST) flat-space instanton and we thus leave the similar further analysis of our paper in the Skyrme model to the future.

In the WSS model [28–30], the properties of chiral symmetry are encoded in the gauge symmetry of the fields living on the D8-branes. The model shows spontaneous chiral symmetry breaking through the merging of the antipodal stacks of D8/$\overline{\text{D8}}$-branes, hence the symmetry group is reduced to $SU(N_f)_V \times U(1)_A \times U(1)_V$. In the context of this holographic model, the pion matrix can be obtained as the holonomy of the gauge field in the holographic direction, and a baryon is realized as an instanton configuration of the gauge field on the D8-branes, where the winding number of the instanton has the natural interpretation as the baryon number. The instanton on the boundary looks like a skyrmion. In this model, the vector mesons are automatically included; they come from the gauge field fluctuations on the D8-branes. A mechanism quite similar in spirit to that of Ref. [25] can be naturally embedded in the WSS model of holographic QCD [31] and the neutron-proton mass splitting is in fact much easier to compute in this setting.

In the second part of this paper, we will look at two different mass splitting effects: The newly found splitting of the moments of inertia, which we computed in the Skyrme model and verified by full numerical computations, and the η-induced splitting that contributes to the neutron-proton mass splitting. In particular, we checked from the Skyrme model that the correction to the moment of inertia that is linear in the pion mass and analytically calculable is, in fact, the leading-order correction at small pion masses. Since the full numerical computation in the WSS model is much more difficult, we trust the analytic result here due to the check in the Skyrme model. The lack of the full numerical computation in the WSS model means, e.g., that we cannot accurately compute the Δ multiplet masses, but we can quite accurately compute their splitting. We will here consider the complete effective Hamiltonian that, unlike the original scenario [31] produces a less symmetric mass spectrum for baryons. The two effects of transfer of

isospin breaking from quarks to the baryon act in different ways; the first is linear and the second is quadratic in j_z. When they are combined, we have a mass splitting between all four states of the Δ multiplet as well as differences among the mass splittings. The splitting between all four states in the Δ multiplet is an m^2 effect, whereas a splitting between the isospin $3/2$ and $1/2$ states (with either sign) is a linear-in-m effect. In the limit of small m, and with our approximations, the rotor is prolate.

The paper is organized as follows. First, we analyze the origin of the splittings in the Skyrme model in Sec. II, followed by a similar analysis for the holographic WSS model in Sec. III. We conclude with a discussion in Sec. IV.

II. SKYRME MODEL, MASS, AND ISOSPIN BREAKING

The Skyrme model is an effective Lagrangian whose degrees of freedom are the pseudo-Goldstone bosons coming from the breaking of chiral symmetry. The degrees of freedom are given compactly in the form of the $SU(N_f)$-valued field $U(x) = e^{i\phi(x)/f_\pi}$, which in the two-flavor case, i.e., $N_f = 2$ reads

$$U(x) = e^{\frac{i\tau^a \pi^a(x)}{f_\pi}}, \tag{2.1}$$

where τ^a, $a = 1, 2, 3$, are the Pauli matrices and f_π is the pion decay constant. Under chiral transformations $SU(2)_L \otimes SU(2)_R$ the field U behaves as follows:

$$U \to V_L U V_R^\dagger, \quad V_L \in SU(2)_L, \quad V_R \in SU(2)_R. \tag{2.2}$$

The left-invariant current is

$$L_\mu = U^\dagger \partial_\mu U \to V_R L_\mu V_R^\dagger, \tag{2.3}$$

and thus transforms only under right-handed transformations.[1]

In addition to the usual quadratic term ($\mathcal{L}_2$) of the nonlinear σ model, the Skyrme model features a quartic contribution in the derivatives known as the Skyrme term ($\mathcal{L}_4$), which is essential to the stability of the soliton, as well as a mass term ($\mathcal{L}_0$) that explicitly breaks chiral symmetry. The complete effective theory Lagrangian thus reads

$$\begin{aligned}\mathcal{L} &= \mathcal{L}_2 + \mathcal{L}_4 + \mathcal{L}_0 \\ &= \frac{f_\pi^2}{4}\mathrm{Tr}(L_\mu L^\mu) + \frac{1}{32e^2}\mathrm{Tr}([L_\mu, L_\nu][L^\mu, L^\nu]) \\ &\quad + \frac{f_\pi^2 c}{2}\mathrm{Tr}(M(U + U^\dagger - 2\mathbb{1}_2)).\end{aligned} \tag{2.4}$$

[1]There exists also a right-invariant current $R_\mu \equiv \partial_\mu U U^\dagger \to V_L R_\mu V_L^\dagger$, which transforms under left-handed transformations. The Skyrme Lagrangian, however, can be equivalently expressed in terms of either L_μ or R_μ and we choose the former.

Here $M \equiv \mathrm{diag}(m_u, m_d)$ is the quark mass matrix which, in the two-flavored case, only contains the *up* and *down* quark masses

$$\begin{aligned}M &= m_q \mathbb{1}_2 + \epsilon m_q \tau^3, \\ m_q &= \frac{1}{2}(m_u + m_d), \qquad \epsilon = \frac{m_u - m_d}{m_u + m_d}.\end{aligned} \tag{2.5}$$

The parameter c is defined such that, in the expansion of $\mathcal{L}_0$, the mass term for the pions is correctly normalized, that is,

$$\begin{aligned}2cm_q &= c(m_u + m_d) \equiv m_{\pi^0}^2 \simeq (139\ \mathrm{MeV})^2, \\ m_q &= 3.45\ \mathrm{MeV}, \qquad \epsilon = -0.34.\end{aligned} \tag{2.6}$$

By inspection of Eq. (2.4) we can tell that no term proportional to ϵ appears at this stage. This is because it would be proportional to the Pauli matrix τ^3, whose trace is identically zero and $U + U^\dagger \propto \mathbb{1}_2$ for $U \in SU(2)$. (This would not be true for three flavors, see, for example, [32,33].)

A. The static skyrmion

The hedgehog *Ansatz* based upon the assumption of maximal symmetry is

$$U(\mathbf{x}) = e^{i\boldsymbol{\tau}\cdot\hat{\mathbf{x}} f(r)} = \cos(f(r))\mathbb{1}_2 + i(\boldsymbol{\tau}\cdot\hat{\mathbf{x}})\sin(f(r)), \tag{2.7}$$

where $r \equiv |\mathbf{x}|$, $\hat{\mathbf{x}} = \mathbf{x}/|\mathbf{x}|$, and $f(r)$ is the profile function of the field. The spherical symmetry implies that any spatial rotation can be compensated by a rotation in isospin space,

$$\begin{aligned}U(R\mathbf{x}) &= \cos(f(r))\mathbb{1}_2 + i(\boldsymbol{\tau}\cdot R\hat{\mathbf{x}})\sin(f(r)) \\ &= \cos(f(r))\mathbb{1}_2 + iA(\boldsymbol{\tau}\cdot\hat{\mathbf{x}})A^\dagger \sin(f(r)),\end{aligned} \tag{2.8}$$

where $R \in SO(3)$, $A \in SU(2)$, and the equality holds when

$$R_{ij} = \frac{1}{2}\mathrm{Tr}(\tau^i A \tau^j A^\dagger). \tag{2.9}$$

When the quark mass is zero, the Skyrme model has two parameters f_π and e. Correspondingly, the mass and the radius of the skyrmion $M_{\mathrm{Sk}} \sim \frac{f_\pi}{e}$, $R_{\mathrm{Sk}} \sim \frac{1}{f_\pi e}$, where $\sim$ here means "scales like." Energy and length rescaling can set these f_π/e and $1/(f_\pi e)$ to unity and hence only the mass parameter changes the theory. More precisely, only the dimensionless mass parameter $\frac{m_{\pi^0}}{f_\pi e}$ (and the corresponding splitting parameter $\frac{\epsilon m_{\pi^0}}{f_\pi e}$) change the theory and hence the solutions.

After substituting the *Ansatz* (2.7) into Eq. (2.4), we obtain the following expression for the skyrmion mass:

$$M_{\mathrm{Sk}}^{\mathrm{static}} = \frac{2\pi f_\pi}{e}\int \mathrm{d}r\, r^2\left[f'^2 + \frac{2\sin^2 f}{r^2} + \frac{\sin^2 f}{r^2}\left(\frac{\sin^2 f}{r^2} + 2f'^2\right) - 2m^2(\cos f - 1)\right], \tag{2.10}$$

where we have rescaled the lengths as $r \to \frac{r}{f_\pi e}$ and defined the dimensionless pion mass parameter

$$m \equiv \frac{m_{\pi^0}}{f_\pi e}. \tag{2.11}$$

The baryon number, which is given by the degree of the map $U(\mathbf{x}): S^3 \mapsto SU(2)$, is given by

$$B = -\frac{2}{\pi}\int \mathrm{d}r \sin^2(f) f'. \tag{2.12}$$

The equation of motion for the skyrmion is found through the minimization of its mass (2.10) and a straightforward derivation yields

$$\left(1 + \frac{2\sin^2 f}{r^2}\right)f'' + \frac{2f'}{r} + \frac{\sin 2f}{r^2}f'^2 - \frac{\sin 2f}{r^2} - \frac{\sin^2 f \sin 2f}{r^4} - m^2 \sin f = 0. \tag{2.13}$$

The solution of Eq. (2.13) has to be found within the functions that satisfy particular boundary conditions. We already know that, at infinity, the U field must be constant and equal to the identity matrix $\mathbb{1}_2$, which implies $f(r \to \infty) \to 0$. On the other hand, in order to provide a skyrmion with unit charge (i.e., unit baryon number), the profile function must also satisfy $f(0) = \pi$. At large distances f is small and the linearization of the equation of motion (2.13) is

$$f'' + \frac{2f'}{r} - \frac{2f}{r^2} - m^2 f = 0 \tag{2.14}$$

and gives the exact asymptotic behavior

$$f(r) = C\frac{mr+1}{r^2}e^{-mr}, \quad r \gg 1, \tag{2.15}$$

which in physical units (before rescaling the length scales) corresponds to $r \gg (f_\pi e)^{-1}$. C is a proportionality constant in front of the linear tail and is related to the nucleon-nucleon-pion coupling by [5]

$$g_{NN\pi} = \frac{8\pi M_{\mathrm{Sk}}}{f_\pi e^2} C. \tag{2.16}$$

1. Numerical solutions

We present some numerical solutions of Eq. (2.13) for various values of the dimensionless mass parameter m of Eq. (2.11). The profile function $f(r)$ is given in Fig. 1 for values of the mass $m = 0.01, 0.05, 0.1, 0.2, 0.3, 0.5$. We will see shortly that the solutions need to be known very precisely up to a very large distance. In particular, up to distances $r \gg 1/m$, which becomes a challenge for numerical methods in a box. Because of the challenging numerical problem, we have decided to adopt the following strategy. We use the shooting method from $r = r_{\mathrm{min}} \ll 1$ with the conditions $f(r_{\mathrm{min}}) = \pi - f_p r_{\mathrm{min}}$ and $f'(r_{\mathrm{min}}) = f_p$ and a second shooting from $r = r_{\mathrm{max}} = 50$ with f and its derivative given by Eq. (2.15). The choice of $r = 50$ is warranted since it is large enough that we can trust the linearized solution (this will become apparent only *a posteriori*), but not large enough to be the cutoff of the integrals, in particular, for the moment of inertia (see below). Next, we adjust f_p and C until the two solutions and their derivatives match at a point in the middle taken to be $r = r_{\mathrm{mid}} := 5$ (this point can be chosen arbitrarily). Knowing the value of C very precisely enables us to perform integrals analytically from $r \in [r_{\mathrm{max}}, \infty)$ using the linearized solution (2.15).

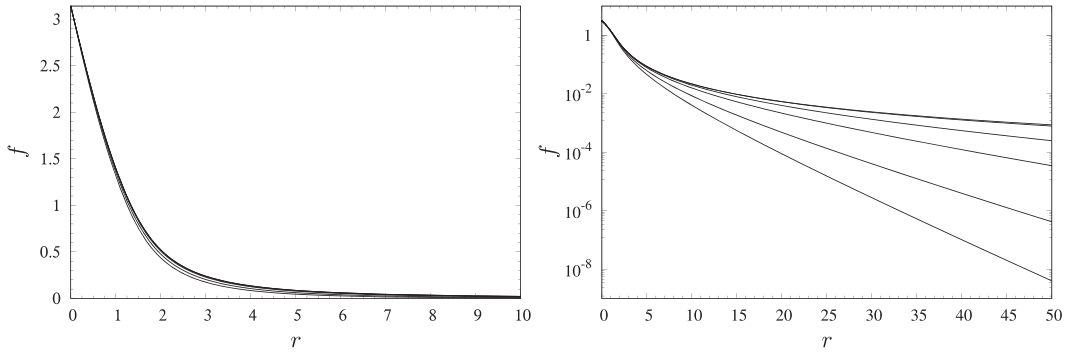

FIG. 1. Profile function $f(r)$ for different values of the mass parameter $m = 0, 0.01, 0.05, 0.1, 0.2, 0.3, 0.5$, corresponding to the curves from top to bottom.

A way to understand and estimate the various parameters is to use Derrick's scaling argument [34], with which we can show that the mass as a function of the radius is given by

$$M(R) = \alpha_2 R + \frac{\alpha_4}{R} + \alpha_0 m^2 R^3, \tag{2.17}$$

where the coefficients $\alpha_{0,2,4}$ come from the mass term, the kinetic term, and the Skyrme term, respectively, and can only be determined numerically from solutions. If we set $m = 0$, minimization of $M(R)$ determines the leading-order Skyrme radius $R_{\rm Sk}(0) = \sqrt{\alpha_4/\alpha_2}$. Minimizing, we get the skyrmion radius

$$R_{\rm Sk}(m)^2 = R_{\rm Sk}(0)^2 \frac{\sqrt{1+8\eta m^2 R_{\rm Sk}(0)^2}-1}{4\eta m^2 R_{\rm Sk}(0)^2}, \quad \eta = \frac{3\alpha_0}{2\alpha_2}. \tag{2.18}$$

Expanding in small m, we obtain

$$R_{\rm Sk}(m) \sim R_{\rm Sk}(0)(1 - \eta m^2 R_{\rm Sk}(0)^2 + \mathcal{O}(m^4)). \tag{2.19}$$

We see that the mass term, to the smallest order, acts as a compressing term shrinking the radius by an order $\sim m^2$. This is confirmed in Fig. 2 where we defined the skyrmion radius by

$$f(R_{\rm Sk}) \simeq 1. \tag{2.20}$$

The soliton shrinks as the mass becomes larger.

The mass of the skyrmion is given in Fig. 3. The mass is increased by a quadratic term for small m and it can be evaluated semianalytically. It is just the action term proportional to m^2 evaluated on the solution obtained at $m = 0$, which we denote as f_0,

$$M_{\rm Sk}^{\rm static}(m) \simeq M_{\rm Sk}^{\rm static}(0) + 4\pi m^2 \int {\rm d}r\, r^2 [(1-\cos f_0)]. \tag{2.21}$$

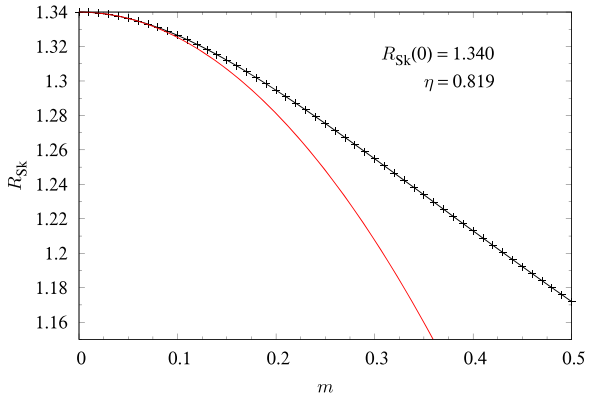

FIG. 2. Skyrmion radius [defined by $f(R_{\rm Sk}) = 1$] as function of m. The red solid curve is a quadratic fit according to Eq. (2.19).

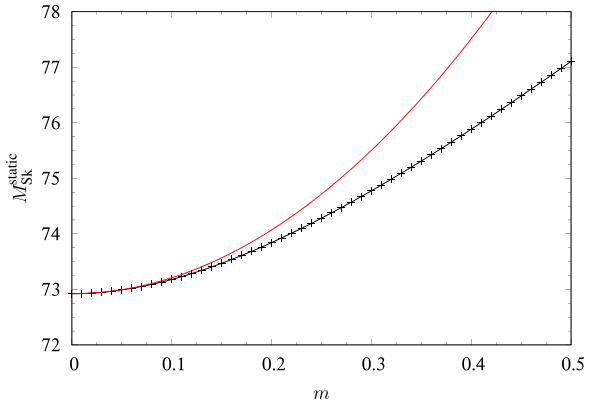

FIG. 3. Skyrmion mass as function of m. The dots show the exact computation and the solid red curve is the quadratic approximation given in Eq. (2.21) computed with the profile function for $m = 0$.

The validity of this approximation is confirmed by the results shown in Fig. 3, where the quadratic behavior characterizes the small-m region of the curve. This type of first-order correction is quite common and is found in many examples [35].

The coefficient $C(m)$ in front of the linear tail is shown in Fig. 4(a). A way to estimate $C(m)$ is the following. If we assume that f is dominated by the linear tail and we write the condition $f(R_{\rm Sk}) = 1$, we have

$$C(m) \frac{1 + m R_{\rm Sk}(m)}{R_{\rm Sk}(m)^2} e^{-m R_{\rm Sk}(m)} \simeq 1. \tag{2.22}$$

Solving for $C(m)$ and expanding to linear order, we obtain

$$C(m) = R(0)^2 + \frac{m^2}{2}(R(0)^4 + 2R(0)R''(0)) + \mathcal{O}(m^3), \tag{2.23}$$

where $R(0) = R_{\rm Sk}(0)$, primes denote derivatives with respect to m, and we have used that $R'(0) = \frac{{\rm d}R}{{\rm d}m}|_{m=0} = 0$, see Eq. (2.19). Inserting the latter equation gives us

$$C(m) = C(0) - 2m^2 C(0)^2 \left(\eta - \frac{1}{4}\right) + \mathcal{O}(m^3),$$
$$C(0) = R(0)^2. \tag{2.24}$$

From the fit shown in Fig. 2 we found that $\eta > 1/4$. This entails that $C(m)$, the coefficient of the linear tail, decreases quadratically with m and that is exactly what we see in Fig. 4(a), where the full numerical solution is presented along with the quadratic fit for small m.

In Fig. 2, the order m^2 correction is well predicted by Eq. (2.24) using the computed value $R(0) = R_{\rm Sk}(0)$, that is the coefficient of m^2 shown in the figure is

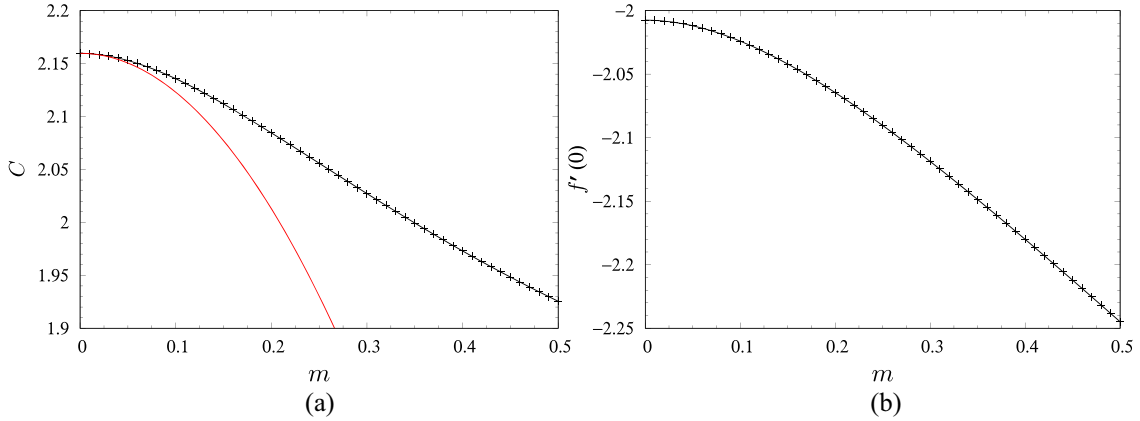

FIG. 4. (a) Coefficient of the linear tail C as function of m. The red curve is the approximation (2.24) with $C(0)$ fitted and η from Fig. 2. (b) The derivative of the profile function at the origin, $f'(0)$.

$-2R(0)^4(\eta - 1/4)$. On the other hand, the prediction of the constant term $C(0) = R(0)^2$ turns out to be a bit coarse as $C(0)$ is computed to be $C(0) = 2.160$, whereas $R(0)^2 = 1.796$ and hence 17% off. Recall that we used rescaled lengths in the discussion above. It will prove convenient to write down the value of the $C(0)$ coefficient in physical units for later comparison,

$$C(0) \simeq \frac{2.160}{(f_\pi e)^2} \simeq 9.99 \times 10^{-6}\,\mathrm{MeV}^{-2} \simeq (0.624\,\mathrm{fm})^2. \quad (2.25)$$

In Fig. 4(b) we show for completeness the other "shooting parameter" for the solution also as a function of m. With the boundary conditions $f(0) = \pi$ and the two parameters C and $f'(0)$, the solution can be reconstructed fully.

We choose the physical values for the pion decay constant and the mass of the uncharged pion, i.e., $f_\pi = 93$ and $m_{\pi^0} = 139$ MeV; the remaining parameter has been set to $e = 5$ according to an estimate given in Ref. [4], which is only slightly different with the older fit, $e = 5.45$ of Ref. [5]. Using $e = 5$ yields $m \simeq 0.3$ as value for the dimensionless pion mass parameter.

Using numerical results for the pion profile function, we obtain the rest mass of the soliton corresponding to both the massless and massive cases (with $m = 0.3$), see Table I. Both results are greater than the average nucleon mass $M_N \simeq 938.9$ MeV of about 44%–48%. We may ask if $m \simeq 0.3$ can be considered small; this depends on the quantity we want to compute. If we consider the mass of the skyrmion, the first-order approximation gives 72.92 while the correct numerical result is 74.78; the approximation (2.21) gives 75.50, thus only 1.0% from the exact result.

TABLE I. Numerical results for the skyrmion mass.

	$M_{\mathrm{Sk}}^{\mathrm{static}}$ (MeV)	Final estimate (MeV)
Massless	$\approx \frac{f_\pi}{e} \times 72.92$	≈1356
Massive ($m = 0.3$)	$\approx \frac{f_\pi}{e} \times 74.78$	≈1391

B. Quantization

To describe baryons, we need to excite the rotational degrees of freedom of the skyrmion. Following Ref. [5], we introduce the $SU(2)$ time-dependent collective variables $A(t)$ such that

$$U(\mathbf{x}, t) = A(t) U_0(\mathbf{x}) A^\dagger(t), \quad (2.26)$$

where $U_0(\mathbf{x})$ is a classical static solution. This corresponds to introducing a rigid isospin rotation, which when quantized corresponds to the isospin quantum number (i.e., the difference between the number of protons and neutrons in a nucleus). Because of the spherical symmetry of the hedgehog *Ansatz*, it is also equivalent to rotation in configuration space by a matrix $R(t)$,

$$U(\mathbf{x}, t) = U_0(R(t)\mathbf{x}), \quad (2.27)$$

which when quantized instead gives rise to the spin quantum number. Obviously, for the spherically symmetric $B = 1$ skyrmion, the spin and isospin quantum numbers must be equal in magnitude. Inserting Eq. (2.26) into Eq. (2.4) we obtain

$$E_{\mathrm{rot}} = \int \mathrm{d}^3x \left[-\frac{f_\pi^2}{4} \mathrm{Tr}(L_0 L_0) - \frac{1}{16e^2} \mathrm{Tr}([L_0, L_i][L_0, L_i]) \right]$$
$$= I \mathrm{Tr}(\dot{A}^\dagger \dot{A}) = \frac{1}{2} I \Omega^2, \quad (2.28)$$

where we have defined the angular velocity Ω so that

$$\frac{\mathrm{i}}{2} \tau \cdot \Omega = -\dot{A} A^\dagger \quad \text{or, equivalently,} \quad \Omega_i = -\frac{1}{2} \epsilon_{ijk} (\dot{R} R^{\mathrm{T}})_{jk}. \quad (2.29)$$

I in Eq. (2.28) is the moment of inertia of the skyrmion and it is an integral functional of the profile function,

$$I = \int \mathrm{d}^3x \mathcal{I} = \left(\frac{1}{f_\pi e^3}\right)\frac{8\pi}{3}\int \mathrm{d}r\, r^2 \sin^2 f\left(1 + f'^2 + \frac{\sin^2 f}{r^2}\right), \tag{2.30}$$

where we have first integrated out the angular dependence using that

$$\int \mathrm{d}\theta \mathrm{d}\varphi\, \sin\theta \hat{x}_i \hat{x}_j = \frac{4\pi}{3}\delta_{ij} \tag{2.31}$$

and rescaled $r \to \frac{r}{f_\pi e}$ as before.

Now we discuss the moment of inertia. The exact function is (2.30). If we assume that f is essentially given by the linear tail, we get

$$I \simeq \frac{8\pi}{3}\int_{R_{\mathrm{UV}}}^{\infty} \mathrm{d}r\, r^2 f^2, \quad f(r) \simeq C(m)\frac{1+mr}{r^2}e^{-mr}. \tag{2.32}$$

The above is only a lower bound on the moment of inertia since we are completely discarding the contribution from the core of the soliton. It is important to put a UV cutoff $R_{\mathrm{UV}} \simeq R_{\mathrm{Sk}}$, first because the linear tail is a good approximation only up to the skyrmion core, and second because this expression would be divergent otherwise. We can then perform the integral obtaining

$$I \simeq \frac{8\pi}{3}C(m)^2 e^{-2mR_{\mathrm{UV}}}\left(\frac{m}{2} + \frac{1}{R_{\mathrm{UV}}}\right). \tag{2.33}$$

The UV divergence is the term $\sim\frac{1}{R_{\mathrm{UV}}}$ and when we put $R_{\mathrm{UV}} \sim R_{\mathrm{Sk}}(m)$ we get exactly the order of magnitude of $I(0)$. Expanding in powers of m we get

$$\begin{aligned} I(m) &= \frac{8\pi}{3}C(0)^2\left(\frac{1}{R_{\mathrm{UV}}} - \frac{3}{2}m + \mathcal{O}(m^2)\right) \\ &= I(0) - 4\pi C(0)^2 m + O(m^2). \end{aligned} \tag{2.34}$$

The coefficient in front of the linear term can be computed exactly, and it is $-4\pi C(0)^2$. This linear behavior with the exact coefficient is confirmed in Fig. 5. It is important to stress the conditions that makes the linear approximation (2.34) computable. There is an m dependence both in $C(m)$ and in $R_{\mathrm{UV}} \sim R_{\mathrm{Sk}}(m)$. This dependence is quadratic as we saw before, so it does not affect the linear term in m. So Eq. (2.34) becomes exactly computable, apart from $C(0)$ that has to be extracted from the numerical solution at $m = 0$.

We compute the integral in Eq. (2.30) for massless and massive pions; the results are listed in Table II. The first-order correction linear in m is a tail effect or, more precisely, due to the "lack of tail." For $0 \neq m \ll 1$, we can consider the solution to be roughly equal to the $m = 0$ solution, up to the scale $r_m \sim \frac{1}{m}$ where everything falls off exponentially. The moment of inertia on the $m = 0$ solution is then reduced by the fact that beyond r_m the field is practically zero. The lack of tail beyond r_m is the reason for the negative linear contribution in m [Eq. (2.34)]. This is quite different in nature than the first-order contribution to the mass [Eq. (2.21)], which is instead due to the unperturbed solution evaluated on the perturbed term and thus is a "core" effect. For a numerical evaluation of the moment of inertia at small mass, it is very important to have a large IR cutoff, at least bigger than the scale r_m. If we consider the inertia of the skyrmion, the correct numerical result is 38.28, and the approximation (2.34) gives 35.80, thus only 6.5% from the correct result; this not as close as what happened for the mass, but we can still consider m small for the computation of I.

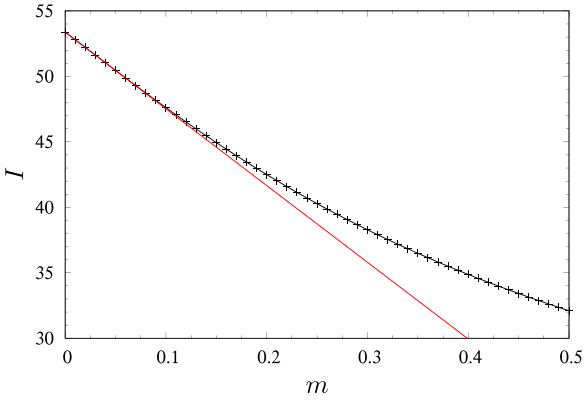

FIG. 5. Moment of inertia for the skyrmion as function of m. The slope of the red solid line computed analytically as $-4\pi C(0)^2$.

The next step is the quantization of the rotational energy. The conjugate classical momentum of the angular velocity Ω is

$$J^i = \frac{\partial E_{\mathrm{rot}}}{\partial \Omega_i} = I\Omega^i,$$

which means that the rotational energy can be re-expressed as

$$E_{\mathrm{rot}} = \frac{J^2}{2I}.$$

TABLE II. Numerical results for the moment of inertia of the skyrmion.

	I (MeV^{-1})	Final estimate (GeV^{-1})
Massless	$\approx\frac{1}{f_\pi e^3}\times 53.38$	≈4.592
Massive	$\approx\frac{1}{f_\pi e^3}\times 38.28$	≈3.293

TABLE III. Matrix elements of $A(t)$ corresponding to the fundamental spinor representation.

	A_{11}	A_{12}	A_{21}	A_{22}
J_3	$1/2$	$-1/2$	$1/2$	$-1/2$
I_3	$-1/2$	$-1/2$	$1/2$	$1/2$
	$\|n\uparrow\rangle$	$\|n\downarrow\rangle$	$\|p\uparrow\rangle$	$\|p\downarrow\rangle$

Following the quantum mechanical rules for the quantization of the angular momentum, we have that the eigenvalues of the total energy or skyrmion mass are

$$M_{\rm Sk} = M_{\rm Sk}^{\rm static} + \frac{1}{2I} j(j+1), \quad j = 0, \frac{1}{2}, 1, \frac{3}{2}, \ldots, \tag{2.35}$$

where we have set $\hbar = 1$. The rigid rotor quantization is valid as long as the energy splitting of the rotational states are much smaller than any vibrational states that deform the rotor. From a theoretical point of view it is always possible to achieve this limit by sending $\hbar \to 0$. Here we will always work in this approximation. Changing to the energy units $\frac{f_\pi}{e}$ and length units $(f_\pi e)^{-1}$, the would-be $\hbar = e^{-2}$. From a phenomenological point of view, we have $e \simeq 5$, so $e^{-2} \simeq 0.04$ which can be considered small.

We can explicitly construct the physical quantities and quantum operators in terms of the parametrization of the $SU(2)$-valued $A(t)$ matrix as [5]

$$A(t) = a_0 \mathbb{1} + \mathrm{i} a_k \tau^k, \quad a_0, a_k \in \mathbb{R}, \text{ and } a_0^2 + a_k^2 = 1. \tag{2.36}$$

The Lagrangian becomes a function of the a's and its temporal derivatives, i.e., $\mathcal{L} = \mathcal{L}(a, \dot{a})$. Using Eq. (2.29), the angular velocity Ω in terms of the local parameters is

$$\Omega_i(a, \dot{a}) = 2(a_i \dot{a}_0 - a_0 \dot{a}_i + \epsilon_{ijk} a_j \dot{a}_k), \tag{2.37}$$

where the nonlinear constraint $a_0^2 + a_k^2 = 1$ has been used to make $\dot{A}A^\dagger$ and hence $\tau \cdot \Omega$ $\mathfrak{su}(2)$ valued, and the conjugate momentum to a_μ is

$$p_\mu = \frac{\partial L}{\partial \dot{a}_\mu} = 4I \dot{a}_\mu, \qquad \mu = 0, 1, 2, 3, \tag{2.38}$$

where p_μ^2 is the Laplacian on the three-sphere [5]. Notice that μ is here not a spacetime index, but is an index on the Euclidean three-sphere and therefore we do not distinguish lower and upper indices. We have all we need to write down the Hamiltonian associated with the rotational modes of the skyrmion, i.e.,

$$H = p_\mu \dot{a}_\mu - L = M_{\rm Sk}^{\rm static} + \frac{1}{8I} p_\mu^2. \tag{2.39}$$

We finally notice that the rotational Lagrangian in Eq. (2.28) is manifestly invariant under two types of $SU(2)$ global transformations, "rotations" and "isorotations," respectively, namely,

$$A(t) \to A(t)B \quad \text{and} \quad A(t) \to BA(t), \quad \text{with} \quad B \in SU(2).$$

The classical charges associated with these transformations can easily be found and they represent the skyrmion's spin and isospin,

$$J_i = \mathrm{i} I \mathrm{Tr}(\tau^i \dot{A} A^\dagger), \; I_i = -\mathrm{i} I \mathrm{Tr}(\tau^i A^\dagger \dot{A}), \; A = A(t), \tag{2.40}$$

or in their quantum operator forms, after using Eq. (2.38) and making the replacement $p_\mu \to -\mathrm{i} \frac{\partial}{\partial a_\mu}$,

$$J_i = -\frac{\mathrm{i}}{2} \left(a_0 \frac{\partial}{\partial a_i} - a_i \frac{\partial}{\partial a_0} + \epsilon_{ijk} a_j \frac{\partial}{\partial a_k} \right), \tag{2.41}$$

$$I_i = -\frac{\mathrm{i}}{2} \left(a_i \frac{\partial}{\partial a_0} - a_0 \frac{\partial}{\partial a_i} + \epsilon_{ijk} a_j \frac{\partial}{\partial a_k} \right). \tag{2.42}$$

We can now classify the matrix element of $A(t)$ in terms of their spin and isospin eigenvalues so to determine the neutron and proton states [5], as shown in Table III, see also Fig. 6. In particular, it can be verified that higher representations can be constructed from monomials in elements of $A(t)$; that is, let $A(t)^l_{ij}$ be the lth power of any matrix element of $A(t)$, then it carries $J = I = l/2$, see Table IV.

In nature, baryons carrying half-integer spin and isospin equal to $1/2$ and $3/2$ are nucleons (n and p) and Δ resonances, respectively. From Eq. (2.35), we can actually give an estimate for their mass [5], i.e.,

$$M_{n,p} = M_{\rm Sk}^{\rm static} + \frac{3}{8I}, \qquad M_\Delta = M_{\rm Sk}^{\rm static} + \frac{15}{8I},$$
$$M_\Delta - M_{n,p} = \frac{3}{2I}, \tag{2.43}$$

TABLE IV. Matrix elements of $A(t)$ corresponding to the Δ representation. Only the positive spins are displayed in this table.

	A_{11}^3	$A_{11}^2 A_{12}$	$A_{11}^2 A_{21}$	$A_{11}^2 A_{22}$ $A_{11} A_{12} A_{21}$	$A_{11} A_{21}^2$ $A_{11} A_{21} A_{22}$	$A_{12} A_{21}^2$	$A_{21}^2 A_{22}$	A_{21}^3
J_3	$3/2$	$1/2$	$3/2$	$1/2$	$3/2$	$1/2$	$1/2$	$3/2$
I_3	$-3/2$	$-3/2$	$-1/2$	$-1/2$	$1/2$	$1/2$	$3/2$	$3/2$
	$\|\Delta_- \uparrow\uparrow\rangle$	$\|\Delta_- \uparrow\rangle$	$\|\Delta_0 \uparrow\uparrow\rangle$	$\|\Delta_0 \uparrow\rangle$	$\|\Delta_+ \uparrow\uparrow\rangle$	$\|\Delta_+ \uparrow\rangle$	$\|\Delta_{++} \uparrow\rangle$	$\|\Delta_{++} \uparrow\uparrow\rangle$

TABLE V. Results for the nucleon and Δ masses. Here the $f_\pi = 93$ MeV, $e = 5$, and the massive case has $m \simeq 0.3$.

	$M_{n,p}$ (MeV)	M_Δ (MeV)	$\frac{M_\Delta - M_{n,p}}{M_{n,p}}$
Massless	≈1438	≈1765	≈0.23
Massive	≈1505	≈1960	≈0.30
Real	≈939	≈1232	≈0.31

with the numerical results summarized in Table V. The model we have studied does still not account for the mass difference between the neutron and the proton, nor for the mass difference between the Δ's. This is due to the fact that no isospin breaking term appears in the Hamiltonian (2.35).

C. Adding the η contribution

The first step to modify the old theory is by enlarging the symmetry group from $SU(2)$ to $U(2)$, that is, also considering the $U(1)$ generator whose corresponding field we shall call η,

$$U = e^{\frac{i\pi^a\tau^a}{f_\pi}} \to U' = Ue^{\frac{i\eta}{f_\pi}} = e^{\frac{i(\pi^a\tau^a+\eta\mathbb{1}_2)}{f_\pi}}, \tag{2.44}$$

where we have set the singlet decay constant equal to f_π, since we are working in the large-N_c expansion setup. The η field corresponds to the generator of the unbroken $U(1)_A$ symmetry group, which produces the axial anomaly. Even in the chiral limit this particle shows a nonvanishing mass, which is directly related to the axial anomaly. The insertion of a phase factor generated by the η field changes the left-invariant current in the following way:

$$L_\mu(\pi) \to L_\mu(\pi) + \frac{i}{f_\pi}\partial_\mu\eta\mathbb{1}_2. \tag{2.45}$$

The Skyrme term $\mathcal{L}_4$ is left unchanged and no η dependence can be present since it only appears as an additional term proportional to the identity matrix. Although the Skyrme term does not change, the other two terms $\mathcal{L}_2$ and $\mathcal{L}_0$ are modified. The new Lagrangian is written in the same way as before. We have chosen not to include the anomaly-related mass of η since, in the limit where $N_c \to \infty$, it vanishes as it is of order $1/N_c$. However, this might not be the case in the real world where $N_c = 3$ and a more detailed and careful analysis may be necessary. We can thus write down the static Lagrangian as

$$\mathcal{L} = -\frac{1}{2}\partial_\mu\eta\partial^\mu\eta + \frac{f_\pi^2}{4}\mathrm{Tr}(L_\mu L^\mu) + \frac{1}{32e^2}\mathrm{Tr}([L_\mu, L_\nu][L^\mu, L^\nu]) + f_\pi^2 m_{\pi^0}^2\left(\sigma\cos\frac{\eta}{f_\pi} - 1\right) - \epsilon f_\pi^2 m_{\pi^0}^2\boldsymbol{\pi}^3\sin\frac{\eta}{f_\pi}, \tag{2.46}$$

where we keep L_μ as the left-invariant current of the $SU(2)$ matrix U and we have conveniently defined

$$U = e^{\frac{i\pi^a\tau^a}{f_\pi}} = \sigma\mathbb{1}_2 + i\boldsymbol{\tau}\cdot\boldsymbol{\pi} = \phi^0\mathbb{1}_2 + i\tau^a\phi^a. \tag{2.47}$$

Notice that the relation between π^a and $\boldsymbol{\pi}^a$ is

$$\boldsymbol{\pi}^a = \frac{\pi^a}{\sqrt{\pi^b\pi^b}}\sin\left(\frac{\sqrt{\pi^c\pi^c}}{f_\pi}\right). \tag{2.48}$$

The mass term now shows an ϵ dependence, strictly related to the "existence" of η. We note that a spherical solution using the *Ansatz* (2.7), for which both $\boldsymbol{\pi}$ and η are just functions of the radius r, cannot yield the newfound breaking term proportional to the quark mass splitting ϵ,

$$\begin{aligned}\epsilon f_\pi^2 m_{\pi^0}^2\int \mathrm{d}^3x\,\boldsymbol{\pi}^3\sin\frac{\eta}{f_\pi} &= 2\pi\epsilon f_\pi^2 m_{\pi^0}^2\int \mathrm{d}r\mathrm{d}\theta\, r^2\sin\theta\cos\theta\sin f(r)\sin\left(\frac{\eta(r)}{f_\pi}\right)\\ &\propto \int_0^\pi \mathrm{d}\theta\,\sin(2\theta) = 0.\end{aligned} \tag{2.49}$$

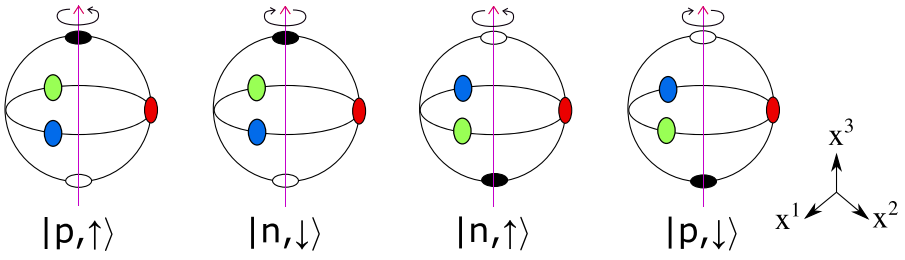

FIG. 6. Schematic representations of the four states corresponding to the fundamental representation of $SU(2)$. The proton spins in both physical and isospin (colors) space in the same direction, whereas the neutron behaves oppositely. The colors are representing the "direction" of the pions wrapping the $SU(2)$ target space, with $\hat{\pi}_1 + i\hat{\pi}_2 = e^{i\theta}$ and $\theta = 0, 2\pi/3, 4\pi/3$ corresponding to red, green, blue, respectively, where $\hat{\pi}^a = \frac{\pi^a}{\pi^b\pi^b}$ is the normalized pion field of Eq. (2.1). White and black correspond instead to the $\hat{\pi}_3 = \pm 1$, respectively. The "classical" version of the spinning nucleons has been discussed in Ref. [37].

We now perform the rescaling $x^\mu \to \frac{x^\mu}{f_\pi e}$ and $\eta \to \eta f_\pi$, obtaining

$$\begin{aligned}\frac{\mathcal{L}}{f_\pi^4 e^2} &= -\frac{1}{2}\partial_\mu\eta\partial^\mu\eta - \frac{1}{2}\partial_\mu\sigma\partial^\mu\sigma - \frac{1}{2}\partial_\mu\boldsymbol{\pi}\cdot\partial^\mu\boldsymbol{\pi} \\ &\quad - \frac{1}{4}(\partial_\mu\sigma\partial^\mu\sigma + \partial_\mu\boldsymbol{\pi}\cdot\partial^\mu\boldsymbol{\pi})^2 \\ &\quad + \frac{1}{4}(\partial_\mu\sigma\partial_\nu\sigma + \partial_\mu\boldsymbol{\pi}\cdot\partial_\nu\boldsymbol{\pi})(\partial^\mu\sigma\partial^\nu\sigma + \partial^\mu\boldsymbol{\pi}\cdot\partial^\nu\boldsymbol{\pi}) \\ &\quad - m^2(1-\sigma\cos\eta) - \epsilon m^2\boldsymbol{\pi}^3\sin\eta. \end{aligned} \tag{2.50}$$

We note that σ is an auxiliary field due to the nonlinear constraint $\sigma^2 + \boldsymbol{\pi}\cdot\boldsymbol{\pi} = 1$. Regarding only $\boldsymbol{\pi}$ as the physical field, we have

$$\sigma = \sqrt{1-\boldsymbol{\pi}\cdot\boldsymbol{\pi}} = 1 - \frac{1}{2}\boldsymbol{\pi}\cdot\boldsymbol{\pi} + \mathcal{O}(\boldsymbol{\pi}^4), \tag{2.51}$$

and therefore we can write down the quadratic Lagrangian as

$$\mathcal{L}^{\text{quad}} = -\frac{1}{2}\partial_\mu\eta\partial^\mu\eta - \frac{1}{2}\partial_\mu\boldsymbol{\pi}\cdot\partial^\mu\boldsymbol{\pi} - \frac{1}{2}m^2(\boldsymbol{\pi}\cdot\boldsymbol{\pi} + \eta^2 + 2\epsilon\boldsymbol{\pi}^3\eta). \tag{2.52}$$

The addition of η has produced an off-diagonal contribution to the mass term, due to the mixing between η and $\boldsymbol{\pi}^3$. The new mass matrix reads

$$M^2 = m^2\begin{pmatrix} 1 & 0 & 0 & 0 \\ 0 & 1 & 0 & 0 \\ 0 & 0 & 1 & \epsilon \\ 0 & 0 & \epsilon & 1 \end{pmatrix}. \tag{2.53}$$

Its eigenvalues in units of m^2 are $1, 1, 1\pm\epsilon$ and the eigenvectors corresponding to the two nonunity eigenvalues are given by $\frac{1}{\sqrt{2}}(\boldsymbol{\pi}^3 \pm \eta)$. The quadratic Lagrangian (2.52) can now be rewritten in terms of $\tilde{\boldsymbol{\pi}} = (\boldsymbol{\pi}^1, \boldsymbol{\pi}^2, \frac{1}{\sqrt{2}}(\boldsymbol{\pi}^3 + \eta), \frac{1}{\sqrt{2}}(\boldsymbol{\pi}^3 - \eta))$ as

$$\mathcal{L}^{\text{quad}} = -\frac{1}{2}\partial_\mu\tilde{\boldsymbol{\pi}}\cdot\partial^\mu\tilde{\boldsymbol{\pi}} - \frac{1}{2}\tilde{\boldsymbol{\pi}}\tilde{M}^2\tilde{\boldsymbol{\pi}}^{\text{T}}, \tag{2.54}$$

where $\tilde{M}^2$ is the diagonal form of M^2,

$$\tilde{M}^2 = m^2\text{diag}(1, 1, 1+\epsilon, 1-\epsilon). \tag{2.55}$$

We want to solve linear equations in a spherical coordinate system that reflects the behavior at large distance. We end up with the following expressions:

$$\begin{aligned}\boldsymbol{\pi}^1 &= C\frac{mr+1}{r^2}e^{-mr}\hat{x}^1, \\ \boldsymbol{\pi}^2 &= C\frac{mr+1}{r^2}e^{-mr}\hat{x}^2, \end{aligned} \tag{2.56}$$

and we obtain for $\boldsymbol{\pi}^3$ and η,

$$\begin{aligned}\boldsymbol{\pi}^3 &= \frac{D}{2}\frac{m\sqrt{1+\epsilon}r+1}{r^2}e^{-m\sqrt{1+\epsilon}r}\hat{x}^3 \\ &\quad + \frac{E}{2}\frac{m\sqrt{1-\epsilon}r+1}{r^2}e^{-m\sqrt{1-\epsilon}r}\hat{x}^3, \\ \eta &= \frac{D}{2}\frac{m\sqrt{1+\epsilon}r+1}{r^2}e^{-m\sqrt{1+\epsilon}r}\hat{x}^3 \\ &\quad - \frac{E}{2}\frac{m\sqrt{1-\epsilon}r+1}{r^2}e^{-m\sqrt{1-\epsilon}r}\hat{x}^3, \end{aligned} \tag{2.57}$$

where C, D, and E are coefficients to be determined and we have used that

$$\begin{aligned}&\partial_i^2(f(r)\hat{x}^a) - m^2 f(r)\hat{x}^a \\ &\quad = \left(f''(r) + \frac{2}{r}f'(r) - \frac{2}{r^2}f(r) - m^2 f(r)\right)\hat{x}^a, \end{aligned} \tag{2.58}$$

and hence $f(r)$ of Eq. (2.15) is a solution to the above equation for any $a = 1, 2, 3$. Now since we want to cover the three-sphere target space, we point each of the pions in the three respective Cartesian directions. In order to let $\boldsymbol{\pi}^3$ be a small perturbation around the expected solution, we choose the fourth tail, i.e., that of $\tilde{\boldsymbol{\pi}}^4$ to be pointed also in the $\hat{x}^3$ direction. This way, $\boldsymbol{\pi}^3$ points purely in the $\hat{x}^3$ direction and is only deformed radially by the presence of nonvanishing ϵ.

For a vanishing quark mass difference, i.e., $\epsilon = 0$, and/or vanishing mass quark m_q, $C = D = E$ and this corresponds to the asymptotic linear tail of the spherically symmetric skyrmion.

The moment of inertia tensor is given by

$$\begin{aligned}\mathcal{I}_{ij} &= \int \mathrm{d}^3x\,\epsilon_{ilm}\epsilon_{jnp}x^l x^n[\partial_m\eta\partial_p\eta + \partial_m\boldsymbol{\pi}\cdot\partial_p\boldsymbol{\pi} \\ &\quad + \partial_m\sigma\partial_p\sigma + (\partial_m\sigma\partial_p\sigma + \partial_m\boldsymbol{\pi}\cdot\partial_p\boldsymbol{\pi})(\partial_k\sigma\partial_k\sigma + \partial_k\boldsymbol{\pi}\cdot\partial_k\boldsymbol{\pi}) \\ &\quad - (\partial_m\sigma\partial_k\sigma + \partial_m\boldsymbol{\pi}\cdot\partial_k\boldsymbol{\pi})(\partial_p\sigma\partial_k\sigma + \partial_p\boldsymbol{\pi}\cdot\partial_k\boldsymbol{\pi})], \end{aligned} \tag{2.59}$$

with the kinetic energy

$$E_{\text{rot}} = \frac{1}{2}\Omega_i\mathcal{I}_{ij}\Omega_j, \tag{2.60}$$

where Ω_i is given in Eq. (2.29) and we have used the fact that under a time-dependent rotation $\mathbf{x} \to R(t)\mathbf{x}$, we have

$$\partial_0\eta(R\mathbf{x}) = \frac{\partial\eta}{\partial(R\mathbf{x})^k}\epsilon_{ijk}(R\mathbf{x})^j\Omega_i, \qquad \Omega_i = -\frac{1}{2}\epsilon_{ijk}(\dot{R}R^{\text{T}})_{jk}. \tag{2.61}$$

Writing the coordinates as $R\mathbf{x} \to \mathbf{x}$ to avoid unnecessary clutter, we arrive at the expression (2.59).

We now proceed with the computation of the moment of inertia of the skyrmion using the linear tail. The strategy is the same we used in Eqs. (2.32)–(2.34) for the spherical skyrmion. The linear tails of the fields are given in Eqs. (2.56) and (2.57). As we are considering only the linear tail, we use only the part of the inertia tensor that comes from the quadratic Lagrangian $\mathcal{L}_2$ [the first line of Eq. (2.59)]. We compute first the contribution from $\boldsymbol{\pi}^3$ that has the form $\boldsymbol{\pi}^3 = \boldsymbol{\pi}^3(r,\theta)$ since it only depends on r and $\hat{x}^3$, obtaining

$$\mathcal{I}_{\pi^3} = \int \mathrm{d}r\mathrm{d}\theta\mathrm{d}\varphi\, r^2 \sin\theta \left(\frac{\partial \boldsymbol{\pi}^3}{\partial\theta}\right)^2 \begin{pmatrix} \sin^2\varphi & 0 & 0 \\ 0 & \cos^2\varphi & 0 \\ 0 & 0 & 0 \end{pmatrix}. \tag{2.62}$$

Integrating over φ and summing the two similar contributions from $\boldsymbol{\pi}^3$ and η we have

$$\mathcal{I}_{\pi^3} + \mathcal{I}_{\eta} = \pi \int \mathrm{d}r d\theta\, r^2 \sin\theta \left(\left(\frac{\partial \boldsymbol{\pi}^3}{\partial\theta}\right)^2 + \left(\frac{\partial\eta}{\partial\theta}\right)^2\right) \begin{pmatrix} 1 & 0 & 0 \\ 0 & 1 & 0 \\ 0 & 0 & 0 \end{pmatrix}. \tag{2.63}$$

Using the asymptotic linear solutions found in Eqs. (2.56) and (2.57) we get

$$\mathcal{I}_{\pi^3} + \mathcal{I}_{\eta} = \frac{8\pi}{3} \int \mathrm{d}r\, r^2 \left(\left(\frac{D}{2}\frac{m\sqrt{1+\epsilon}r+1}{r^2} e^{-m\sqrt{1+\epsilon}r}\right)^2 + \left(\frac{E}{2}\frac{m\sqrt{1-\epsilon}r+1}{r^2} e^{-m\sqrt{1-\epsilon}r}\right)^2\right) \begin{pmatrix} 1 & 0 & 0 \\ 0 & 1 & 0 \\ 0 & 0 & 0 \end{pmatrix}. \tag{2.64}$$

Using the asymptotic linear solutions found in Eqs. (2.56) and (2.57), the contributions from $\boldsymbol{\pi}^1$ and $\boldsymbol{\pi}^2$ are

$$\mathcal{I}_{\pi^1} + \mathcal{I}_{\pi^2} = \frac{4\pi}{3} \int \mathrm{d}r\, r^2 \left(C\frac{mr+1}{r^2} e^{-mr}\right)^2 \begin{pmatrix} 1 & 0 & 0 \\ 0 & 1 & 0 \\ 0 & 0 & 2 \end{pmatrix}. \tag{2.65}$$

Summing over all contributions, we finally obtain the total inertia tensor

$$\mathcal{I} = \mathcal{I}_{\pi^1} + \mathcal{I}_{\pi^2} + \mathcal{I}_{\pi^3} + \mathcal{I}_{\eta}. \tag{2.66}$$

The inertia tensor can be split into an identity part and a deformation,

$$\mathcal{I} = I\mathbb{1}_3 + \delta \begin{pmatrix} 1 & 0 & 0 \\ 0 & 1 & 0 \\ 0 & 0 & -2 \end{pmatrix}. \tag{2.67}$$

The moment of inertia of the resulting skyrmion may be more oblate like a pancake or more prolate like an American football, depending on the sign of δ. For $\epsilon = 0$ and $C = D = E$, we obtain $\delta = 0$ and

$$I = \frac{8\pi}{3} \int \mathrm{d}r\, r^2 C^2 \left(\frac{mr+1}{r^2} e^{-mr}\right)^2, \tag{2.68}$$

which is the result of Eq. (2.32) for the spherical case.

These integrals, as in the spherical case, are UV divergent. As before, these solutions are valid up to a UV cutoff R_{UV} where the solution becomes nonlinear; R_{UV} is essentially the size of the skyrmion R_{Sk}. Integrating over r from the UV cutoff, we obtain

$$\mathcal{I} = \frac{4\pi}{3} C(m)^2 e^{-2mR_{\mathrm{UV}}} \left(\frac{m}{2} + \frac{1}{R_{\mathrm{UV}}}\right) \begin{pmatrix} 1 & 0 & 0 \\ 0 & 1 & 0 \\ 0 & 0 & 2 \end{pmatrix} + \frac{2\pi}{3} \left[D(m)^2 e^{-2m\sqrt{1+\epsilon}R_{\mathrm{UV}}} \left(\frac{m\sqrt{1+\epsilon}}{2} + \frac{1}{R_{\mathrm{UV}}}\right) + E(m)^2 e^{-2m\sqrt{1-\epsilon}R_{\mathrm{UV}}} \left(\frac{m\sqrt{1-\epsilon}}{2} + \frac{1}{R_{\mathrm{UV}}}\right)\right] \begin{pmatrix} 1 & 0 & 0 \\ 0 & 1 & 0 \\ 0 & 0 & 0 \end{pmatrix}. \tag{2.69}$$

Expanding in m yields a UV divergent term $\propto 1/R_{\mathrm{UV}} \sim 1/R_{\mathrm{Sk}}$,

$$\mathcal{I} = \frac{4\pi}{3}\frac{C(0)^2}{R_{\rm UV}}\begin{pmatrix}1&0&0\\0&1&0\\0&0&2\end{pmatrix} + \frac{2\pi}{3}\frac{(D(0)^2+E(0)^2)}{R_{\rm UV}}\begin{pmatrix}1&0&0\\0&1&0\\0&0&0\end{pmatrix} - 2\pi C(0)^2 m\begin{pmatrix}1&0&0\\0&1&0\\0&0&2\end{pmatrix} - \pi\left(\sqrt{1+\epsilon}D(0)^2+\sqrt{1-\epsilon}E(0)^2\right)m\begin{pmatrix}1&0&0\\0&1&0\\0&0&0\end{pmatrix} + \mathcal{O}(m^2,m^2\epsilon), \tag{2.70}$$

where we have assumed that $C'(0) = D'(0) = E'(0) = 0$. Composing the tensor into the diagonal and the eighth Gell-Mann generator according to Eq. (2.67), we get

$$I = \frac{4\pi}{9}\frac{D^2+E^2+4C^2}{R_{\rm UV}} - \frac{2\pi}{3}\left(\sqrt{1+\epsilon}D^2+\sqrt{1-\epsilon}E^2+4C^2\right)m + \mathcal{O}(m^2,m^2\epsilon), \tag{2.71}$$

$$\delta = \frac{2\pi}{9}\frac{D^2+E^2-2C^2}{R_{\rm UV}} - \frac{\pi}{3}\left(\sqrt{1+\epsilon}D^2+\sqrt{1-\epsilon}E^2-2C^2\right)m + \mathcal{O}(m^2,m^2\epsilon), \tag{2.72}$$

where in the above expressions $C = C(0)$, $D = D(0)$, and $E = E(0)$ and $R_{\rm UV}$ can be approximated by $R_{\rm Sk}$.

If we set $D(0) = E(0) = C(0)$, the tensor simplifies as

$$I = \frac{8\pi}{3}\frac{C(0)^2}{R_{\rm UV}} - \frac{2\pi}{3}C(0)^2\left(4+\sqrt{1+\epsilon}+\sqrt{1-\epsilon}\right)m + \mathcal{O}(m^2,m^2\epsilon), \tag{2.73}$$

$$\delta = \frac{\pi}{3}C(0)^2\left(2-\sqrt{1+\epsilon}-\sqrt{1-\epsilon}\right)m + \mathcal{O}(m^2,m^2\epsilon,m\epsilon^4), \tag{2.74}$$

which is difficult to establish without knowledge of the full nonlinear solutions. Expanding the square roots in the linear term of I, we obtain

$$I(m) = I(0) - 4\pi C(0)^2\left(1-\frac{\epsilon^2}{24}\right)m + \mathcal{O}(m^2,m^2\epsilon,m\epsilon^4), \tag{2.75}$$

$$\delta = \frac{\pi}{12}C(0)^2\epsilon^2 m + \mathcal{O}(m^2,m^2\epsilon,m\epsilon^4). \tag{2.76}$$

One could make the assumption that $|\boldsymbol{\pi}^1|_{r=R_{\rm UV}} \simeq |\boldsymbol{\pi}^2|_{r=R_{\rm UV}} \simeq |\boldsymbol{\pi}^3|_{r=R_{\rm UV}}$ and $|\eta|_{r=R_{\rm UV}} \ll |\boldsymbol{\pi}^3|_{r=R_{\rm UV}}$; the latter assumption is equivalent with assuming $D \sim E$. Equating the magnitudes of the tails

$$\begin{aligned} C(m)\frac{mR_{\rm Sk}+1}{R_{\rm Sk}^2}e^{-mR_{\rm Sk}} &\simeq D(m)\frac{m\sqrt{1+\epsilon}R_{\rm Sk}+1}{R_{\rm Sk}^2}e^{-m\sqrt{1+\epsilon}R_{\rm Sk}} \\ &\simeq E(m)\frac{m\sqrt{1-\epsilon}R_{\rm Sk}+1}{R_{\rm Sk}^2}e^{-m\sqrt{1-\epsilon}R_{\rm Sk}}, \end{aligned} \tag{2.77}$$

which when expanding to second order in m yields

$$D - C \simeq \frac{1}{2}m^2\epsilon R_{\rm Sk}^2 C, \quad E - C \simeq -\frac{1}{2}m^2\epsilon R_{\rm Sk}^2 C. \tag{2.78}$$

Plugging this approximation into Eqs. (2.71) and (2.72), we obtain exactly the results (2.75) and (2.76), with the order m^0-terms generating $m^4\epsilon$ corrections and the order m-terms generating $m^3\epsilon$ corrections, all of which we neglect to leading order. This shows that the results (2.75) and (2.76) are quite robust.

Note that the order m correction to I is insensitive to the cutoff $R_{\rm Sk}$ unlike the leading-order term; we can therefore trust the coefficient in front of this linear-in-m term. Notice also that we need to take ϵ^2 into account, but we have expanded only to the first order in m. This is consistent in the limit

$$m \ll |\epsilon|. \tag{2.79}$$

In reality, the physical parameters are $m \simeq 0.3$ and $\epsilon = -0.34$, so for I one should also take the higher-order correction terms of order m^2 and $m^2\epsilon$ into account, which, however, are more complicated expressions and will depend also on the double derivatives $C''(0)$, $D''(0)$, and $E''(0)$.

The form of the inertia tensor is that of Eq. (2.67). This is an axially symmetric rotor; it may be oblate or prolate according to whether δ is negative or positive. The related quantum Hamiltonian becomes then

$$\begin{aligned} H_{\rm rot} &= \frac{1}{2}\mathcal{I}_{ij}^{-1}J_iJ_j = \frac{1}{2}\frac{J^2}{I+\delta} + \frac{1}{2}J_3^2\left[\frac{1}{I-2\delta}-\frac{1}{I+\delta}\right] \\ &= \frac{1}{2}\frac{1}{I+\delta}j(j+1) + \frac{3}{2}\frac{\delta}{(I+\delta)(I-2\delta)}j_3^2, \end{aligned} \tag{2.80}$$

where $j(j+1)$ and j_3 are the eigenvalues of the J^2 and J_3 operators, respectively. Equation (2.80) distinguishes between different values of $j_3 \in [-j, \ldots, j]$ but not their sign, so the states that correspond to the fundamental representation with $j = 1/2$ are left degenerate, i.e., the proton and the neutron have the same mass. The $j = 3/2$ ones instead get split into two pairs (i.e., Δ^{++} and Δ^{-} with $|j_3| = 3/2$, whereas Δ^{+} and Δ^{0} with $|j_3| = 1/2$),

$$M_{\Delta^{++},\Delta^{-}} - M_{\Delta^{+},\Delta^{0}} = \frac{1}{2}(M_{\Delta^{++}} - M_{\Delta^{+}} - M_{\Delta^{0}} + M_{\Delta^{-}}), \tag{2.81}$$

where for the spin Hamiltonian (2.80) we have

$$M_{\Delta^{++},\Delta^{-}} = M_{\Delta^{++}} = M_{\Delta^{-}} = M_{\mathrm{Sk}}^{\mathrm{static}} + H_{\mathrm{rot}}\big|_{j=\frac{3}{2},|j_3|=\frac{3}{2}}, \tag{2.82}$$

$$M_{\Delta^{+},\Delta^{0}} = M_{\Delta^{+}} = M_{\Delta^{0}} = M_{\mathrm{Sk}}^{\mathrm{static}} + H_{\mathrm{rot}}\big|_{j=\frac{3}{2},|j_3|=\frac{1}{2}}, \tag{2.83}$$

since H_{rot} of Eq. (2.80) does not distinguish between j_3 positive and negative, whereas $M_{\mathrm{Sk}}^{\mathrm{static}}$ is the static soliton mass. In particular,

$$\frac{1}{2}(M_{\Delta^{++}} - M_{\Delta^{+}} - M_{\Delta^{0}} + M_{\Delta^{-}}) = \frac{3\delta}{(I+\delta)(I-2\delta)} \simeq \frac{3\delta}{I^2}. \tag{2.84}$$

Assuming the previous results are valid, we get

$$\frac{1}{2}(M_{\Delta^{++}} - M_{\Delta^{+}} - M_{\Delta^{0}} + M_{\Delta^{-}}) \simeq \frac{\pi C(0)^2 m}{I^2}\left(2 - \sqrt{1+\epsilon} - \sqrt{1-\epsilon}\right). \tag{2.85}$$

For the numerical values $m \simeq 0.3$ and $\epsilon \simeq -0.34$, we obtain

$$\frac{1}{2}(M_{\Delta^{++}} - M_{\Delta^{+}} - M_{\Delta^{0}} + M_{\Delta^{-}}) \simeq f_\pi e^3 4.6 \times 10^{-5} \simeq 0.54\ \mathrm{MeV}. \tag{2.86}$$

Note that, in the small-m limit, the linear deviation (2.74) (positive δ) makes the rotor prolate, thus Δ^{++} and Δ^{-} have a higher mass. At a finite but not small m, this may change and only a numerical computation can tell if it is oblate or prolate; in fact, see below. We saw that the small-m condition is very good for the quantity I. For δ we have to be more careful, because also the condition (2.79) has to be respected. So the core contribution to the splitting may be important for the phenomenological values of m and ϵ.

We will now turn to the numerical computation of the Skyrme model with the η taken into account. We use the numerical method developed for the ω-Skyrme model in Ref. [36], where we solve the equation of motion for the scalar η using the conjugate gradients method at every step and solve the nonlinear equation of motion for the pions and the σ using arrested Newton flow. The simplicity of the η equation and the fact that η is not normalized, unlike the fact that $\sigma^2 + \boldsymbol{\pi}^2 = 1$ (coming from $\det U = 1$), makes the conjugate gradients method very efficient. The arrested Newton flow is implemented with a second-order real-time evolution of the field equations (ignoring the time dependence in the Skyrme term), monitoring the (static) potential energy at every step and setting all time derivatives to zero when the potential energy increases with respect to the previous step. This method implies that the fields are accelerating down toward the minimal energy solution, but are "gradient flowing" up to the minimum. The specific implementation of the method was done in CUDA C for NVIDIA GPUs and the lattice was chosen as a 160^3 cubic lattice with step size 0.088 and a five-point fourth-order finite difference stencil for the derivatives.

The small-m limit makes the numerics very hard compared to the usual physical case of a finite pion mass parameter, often taken to be of order one, ensuring a fast exponential decay and allowing numerical computations with finite differences to be put on a finite box without loss of precision. Instead, we consider the numerics for m in the range between typical physical values and all the way down to zero, calling for a modification of the usual methods. We implement Dirichlet boundary conditions on a sufficiently large box, dictated by the linearized exact solutions (2.56) and (2.57) and using as an initial guess the values $C = D = E$ with C from the spherically symmetric case of the previous section. By trial and error, we observe that only after a long simulation time do the derivatives converge to their expected values dictated by Eqs. (2.56) and (2.57); hence, we simply read off the coefficients C, D, and E from the derivatives at the end of the simulation and start it again with the updated values of the coefficients of the tails of the fields. Iterating about 5 times gives a reasonably good precision on the coefficients and the result is shown in Fig. 7. First, we observe that the behavior of the coefficients is quadratic in m for small m, as expected from the spherically symmetric case. Second, we confirm that $C(0) = D(0) = E(0)$ as it should be (since $m = 0$ turns off any splitting, viz. there are no factors of ϵ without at least one power of m). Third, we can confirm that the predicted splitting of the coefficients follow Eq. (2.78), i.e., that $E > C > D$ for $m > 0$ (recall that $\epsilon < 0$). The magnitude of the splitting is, however, not accurate (see the yellow and red dashed lines in Fig. 7).

Since we cannot perform the numerical computations of sufficiently large lattices in order to capture the accurate moment of inertia tensor in the limit of small m, we compute the moment of inertia tensor on the largest sphere fitting into the lattice and calculate the contribution from the outside by using the tails (2.56) and (2.57) and the coefficients of Fig. 7—the latter part is semianalytic,

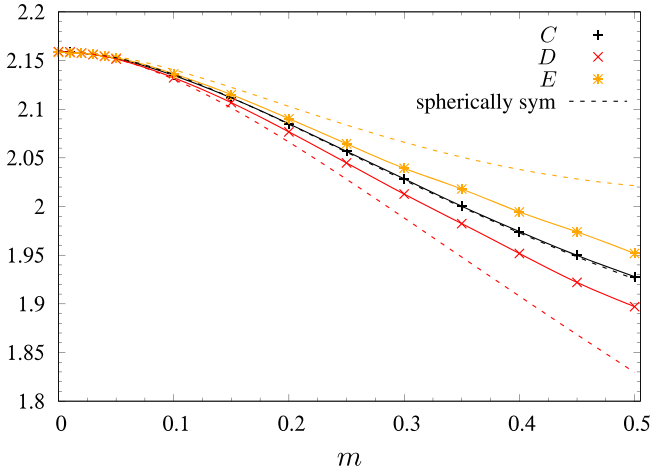

FIG. 7. The coefficients (2.56) and (2.57) of the exponential tails of the pion and η fields as functions of m. The black dashed curve is the result of the spherically symmetric skyrmion (for which there is only one coefficient C of all the three pions), whereas the yellow (upper) and red (lower) dashed curves are the prediction (2.78), which is correct in sign, but not quite in magnitude. In this figure $\epsilon = -0.34$, i.e., its physical value.

although we have to compute the $r-\theta$ integral numerically too.

We confirm that the linear prediction of both the trace part as well as the splitting part (δ) of the moment of inertia tensor is in accord with Eqs. (2.73) and (2.74), at least up to numerical accuracy and order m^2 corrections, see Fig. 8. From the result that δ is everywhere positive, we can conclude for the range of m studied here that the nucleon is always prolate.

We plot the total energy density of the numerical computation with the spin contribution to the energy corresponding to the nucleon, in Fig. 9, where the total energy density in dimensionless units is defined as

$$\mathcal{E}^{\text{tot}} = -\frac{e}{f_\pi}\mathcal{L} + \frac{e^4}{2}\left(\frac{j(j+1)\mathcal{I}_{11}}{I_{11}^2} + \frac{j_3^2\mathcal{I}_{33}}{I_{33}^2} - \frac{j_3^2\mathcal{I}_{11}}{I_{11}^2}\right), \tag{2.87}$$

with $-\mathcal{L}$ of Eq. (2.50), $\mathcal{I}_{ij}$ of Eq. (2.59), $I_{ij} = \int \mathrm{d}^3x \mathcal{I}_{ij}$, and for the nucleon $j = |j_3| = \frac{1}{2}$. This energy density is constructed such that its integral gives the energy of the quantized Hamiltonian (2.80) plus the classical skyrmion mass. From this figure, the nucleon appears to be prolate, but this is the shape of the energy density near the core of the skyrmion/nucleon. We find the same shape for the Δ's. In Fig. 10, we plot the three diagonal components of the inertia tensor density of the skyrmion, which are all tori about their corresponding axis; e.g., the $\mathcal{I}_{11}$ component takes the shape of a torus with the main axis in the x^1 direction and so on. In the right panel of the figure, we show the (y,z) plane of the $\mathcal{I}_{11}$ component with the (x,y) plane of the $\mathcal{I}_{33}$ component of the inertia tensor density subtracted off. This latter panel illustrates that, far from the core, the tail effect of the $\mathcal{I}_{11}$ (and $\mathcal{I}_{22}$ is similar) gives a larger positive relative contribution (in yellow) than the $\mathcal{I}_{33}$ gives a negative relative contribution (in blue). The combined effect is that the tail of the skyrmion makes it prolate. This effect dominates the oblate property of the core.

The presence of the new η particle has affected the skyrmion quite a bit, but we still cannot obtain the mass splitting between the neutron and the proton.

By making the spin-isospin association, as in the hedgehog example, we can infer that the residual neutron-proton symmetry we just found is strictly related to how the skyrmion rotates. Equation (2.80) reveals that any left or right rotating skyrmion has the same energy, which instantly translates into the proton and the neutron being the same soliton solution rotating in opposite directions.

The shape of the resulting skyrmion is obviously dependent upon who wins, but besides that nothing

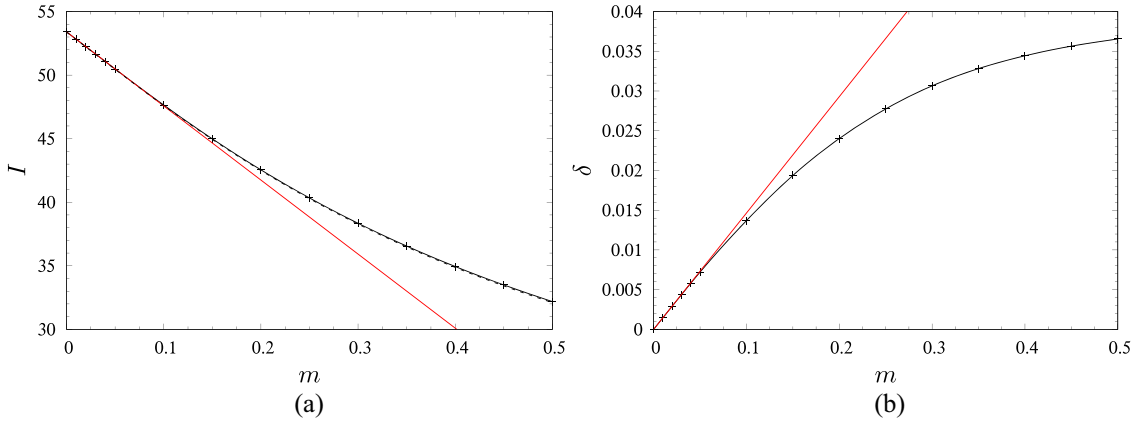

FIG. 8. (a) The trace part and (b) the traceless part [proportional to the Gell-Mann λ^8 generator, see Eq. (2.67)] of the moment of inertia tensor as a function of m computed by a full three-dimensional computation on the lattice with the contribution from outside the lattice to infinity computed from the linearized tail solutions. The red straight lines are the predictions of Eqs. (2.73) and (2.74), respectively, for (a) and (b).

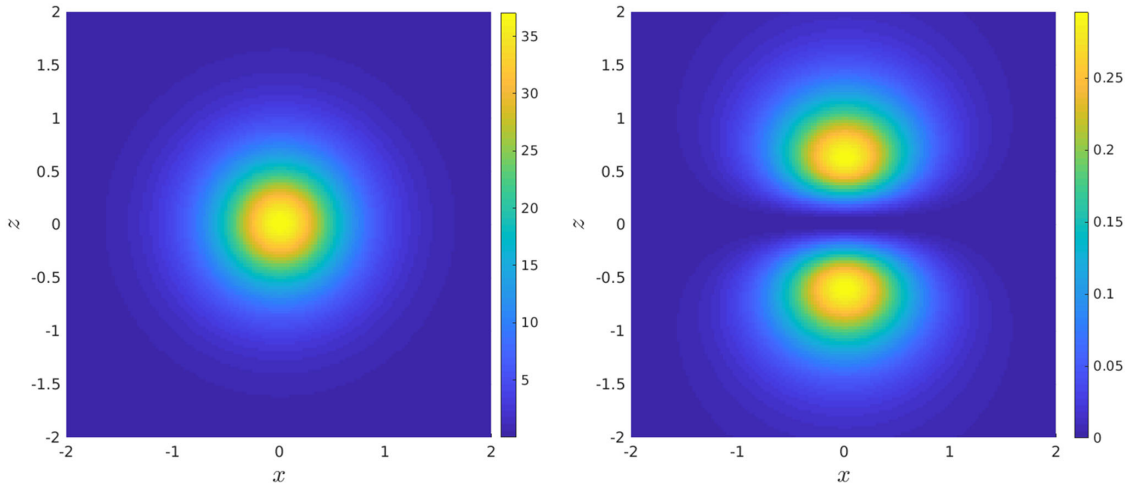

FIG. 9. Left: the energy density $\mathcal{E}^{\mathrm{tot}}(x,0,z)$ of the nucleon, i.e., the energy with spin contribution corresponding to $j = j_3 = 1/2$. Right: $\mathcal{E}^{\mathrm{tot}}(x,0,z)$–$\mathcal{E}(x,y,0)$. In this figure, $m = 0.3$ and $\epsilon = -0.34$.

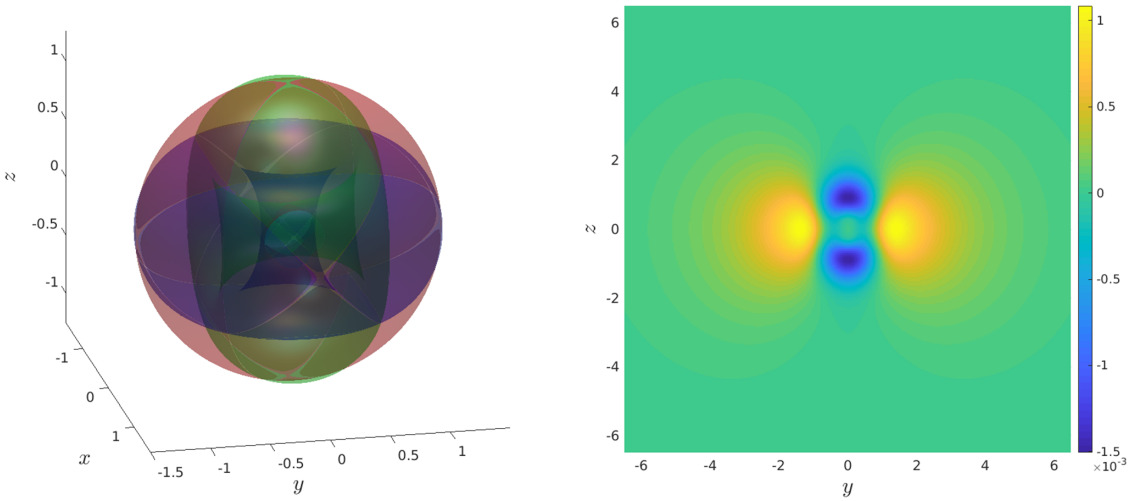

FIG. 10. Left: the three diagonal components of the moment of inertia tensor density $\mathcal{I}_{ii}$ with $i = 1, 2, 3$ (not summed over) shown in red, green, and blue, respectively. Right: $\mathcal{I}_{11}(x,0,z)$–$\mathcal{I}_{33}(x,y,0)$. In this figure $m = 0.3$ and $\epsilon = -0.34$.

changes the fact that the neutron and the proton do not get different masses, as they are the same state rotating in different $SU(2)_I$ directions, as illustrated in Fig. 11. We shall later come back to these terms along with all the others, which give an extra contribution to the moment of inertia; however, for now we should finally address the latter approach, where the splitting is coming from vector mesons.

The persistence of the degeneracy of the neutron-proton multiplet, or, in general, of all the states with the same $|I_3|$, can also be understood by a more general symmetry argument. The Lagrangian with the pions η and the mass splitting breaks the continuous isospin but leaves invariant a discrete isospin parity, for example, as the reflection $R_{\mathrm{iso},13}$: $U \to U^{\mathrm{T}}$ which acts as $(\pi^1, \pi^2, \pi^3) \to (\pi^1, -\pi^2, \pi^3)$. To pass from the proton to the neutron with both spin-up (see the first line of Fig. 11) we can use two symmetry transformations, a space parity P_{spc}: $(x^1, x^2, x^3) \to (-x^1, -x^2, -x^3)$ combined with the isospin parity $R_{\mathrm{iso},13}$. These discrete symmetries protect the degeneracy. This symmetry argument works independent of the various approximations made above, for example, the rigid rotor and the semiclassical quantization.

III. ISOSPIN SPLITTING IN THE WITTEN-SAKAI-SUGIMOTO MODEL

Isospin multiplets turn out to be completely degenerate if we include only pions in such effective theory with $N_f = 2$, while it is possible to have a partial mass splitting between the Δ's if we add the η meson. To completely remove the degeneracy, obtaining also a splitting in mass between the nucleon states, i.e., the proton and the neutron, the inclusion of vector mesons is decisive. The Sakai-Sugimoto

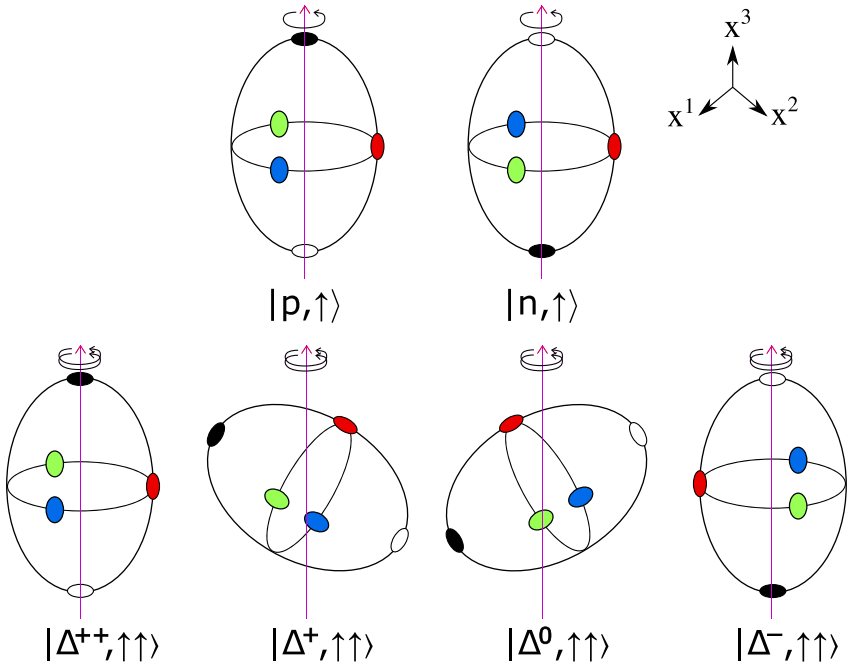

FIG. 11. Schematic representations of the different states corresponding to the fundamental and Δ representation of $SU(2)$, all with maximal spin-up, with the modification of shape due to cylindrical symmetry of the solutions. The colors are the same as in Fig. 6.

model [29,30] has the advantage of automatically including all vector fields and their excitations in a consistent way. Thus, it can account for the presence of the neutron-proton mass splitting incorporating the effect previously considered in Refs. [23–25,27]. Our aim is to incorporate both effects on the Δ's—the one studied in Ref. [31] that also produced the proton-neutron mass splitting, and the one developed in Sec. II due to the splitting of the moments of inertia—and see the complete splitting of the spectrum of Δ's.

We briefly present the baryons in the Sakai-Sugimoto holographic model. We focus on the low-energy flavor dynamics on the fixed metric background in five dimensions, as presented in Refs. [38,39]. The gauge fields on the D8-branes are expanded on the $U(2)$ basis as

$$\mathcal{A} = \hat{A}\frac{\mathbb{1}_2}{2} + A^a\frac{\tau^a}{2}, \qquad \mathcal{F} = \hat{F}\frac{\mathbb{1}_2}{2} + F^a\frac{\tau^a}{2}. \tag{3.1}$$

The 5D reduced metric and the effective action are given by

$$\mathrm{d}s^2 = \frac{1}{h(z)^2}\mathrm{d}x^\mu \mathrm{d}x_\mu + h(z)^2\mathrm{d}z^2, \tag{3.2}$$

$$S_{D8} = -\kappa \mathrm{Tr}\int \mathrm{d}^4x\mathrm{d}z\left[k(z)\mathcal{F}_{\mu z}\mathcal{F}^{\mu z} + \frac{1}{2}h(z)\mathcal{F}_{\mu\nu}\mathcal{F}^{\mu\nu}\right] + S_{\mathrm{CS}}, \tag{3.3}$$

with $h(z)$, $k(z)$ being two functions who play the role of warp factors amounting to

$$k(z) = 1 + z^2, \qquad h(z) = \frac{1}{(1+z^2)^{1/3}}. \tag{3.4}$$

We can see that on the D8-brane's world volume lives a five-dimensional Yang-Mills gauge theory with nontrivial warp factors. It will sometimes be useful to see the explicit N_c dependence of the overall constant of the action, hence we define

$$\kappa = a\lambda N_c, \qquad a = \frac{1}{216\pi^3}. \tag{3.5}$$

The Chern-Simons action has the explicit expression

$$S_{\mathrm{CS}} = \frac{N_c}{384\pi^2}\epsilon^{\alpha_1\alpha_2\alpha_3\alpha_4\alpha_5} \times \int \mathrm{d}^4x\mathrm{d}z\,\hat{A}_{\alpha_1}\left[3F^a_{\alpha_2\alpha_3}F^a_{\alpha_4\alpha_5} + \hat{F}_{\alpha_2\alpha_3}\hat{F}_{\alpha_4\alpha_5}\right]. \tag{3.6}$$

Everything is in the dimensional units of the Kaluza-Klein compactification scale M_{KK}, so the model has two dimensionless couplings: N_c and λ (or κ) and a mass scale M_{KK}.

The holonomy of the $\mathcal{A}_z$ field can be interpreted as the pseudoscalar matrix in a chiral theory [29], so that we will adopt the following definitions:

$$\mathcal{P}\exp\left(\frac{\mathrm{i}}{2}\int \mathrm{d}z\hat{A}_z\right) \equiv e^{\mathrm{i}\varphi(x)},$$
$$\mathcal{P}\exp\left(\mathrm{i}\int \mathrm{d}zA_z\right) \equiv U(x). \tag{3.7}$$

Finally, the model can be supplemented with quark masses via the inclusion of the Aharony-Kutasov action [40],

$$S_{\mathrm{AK}} = c\int \mathrm{d}^4x\,\mathrm{Tr}\mathcal{P}\left[Me^{\mathrm{i}\int \mathrm{d}z\mathcal{A}_z} - \mathbb{1}_2 + \mathrm{H.c.}\right]. \tag{3.8}$$

Note that action (3.8) exhibits nonlocality in the holographic direction. M is the quark mass matrix and c is a constant (related to the chiral condensate) that we can fix to reproduce the expected chiral perturbation theory Lagrangian: This parameter is determined using the pion mass as an input by the Gell-Mann-Oakes-Renner relation

$$c(m_u + m_d) = \frac{1}{2}f_\pi^2 m^2, \tag{3.9}$$

with f_π being the pion decay constant and m the pion mass in units of M_{KK}. Employing definitions (3.7) we can cast the quark mass action into the form

$$S_{\mathrm{AK}} = c\int \mathrm{d}^4x\,\mathrm{Tr}[Me^{\mathrm{i}\varphi}U - \mathbb{1}_2 + \mathrm{H.c.}]. \tag{3.10}$$

This is exactly the same as we had for the Skyrme model. In fact, from the point of view of the quark mass and mass splittings, the Skyrme model and the WSS model are exactly the same, with the caveat that in the WSS model vector mesons and the η are automatically included, and the couplings are fixed by the two free parameters λ, M_{KK}. In the Skyrme truncation of the model, we have [29]

$$\frac{\kappa}{\pi} = \frac{f_\pi^2}{4}, \qquad \frac{\kappa c_S}{2} = \frac{1}{32e^2}, \qquad c_S \simeq 0.156. \tag{3.11}$$

One popular way to calibrate the parameters with mesons is

$$\begin{aligned} &M_{\mathrm{KK}} = 949\ \mathrm{MeV}, \qquad \kappa = 0.00745, \\ &N_c = 3, \qquad \lambda = 16.63. \end{aligned} \tag{3.12}$$

This calibration is done by fitting the ρ-meson mass $M_\rho = 776$ MeV and the pion decay constant $f_\pi = 92.4$ MeV. This mesonic fit is, however, not the only possibility, and in particular, it overestimates masses in the baryon sector.

In the context of this holographic model, a baryon is realized as an instantonic configuration of the gauge field $\mathcal{A}$. The BPST instanton is given by

$$A_M = -\mathrm{i}f(\xi)g\partial_M g^{-1}, \tag{3.13}$$

where we have introduced the following functions:

$$f(\xi) = \frac{\xi^2}{\xi^2+\rho^2}, \qquad g(\mathbf{x},z) = \frac{(z-Z) - \mathrm{i}(\mathbf{x}-\mathbf{X})\cdot\boldsymbol{\tau}}{\xi}, \tag{3.14}$$

the radial coordinate in three space including the holographic direction, i.e., the $(\mathbf{x},z)$ space,

$$\xi = \sqrt{(\mathbf{x}-\mathbf{X})^2 + (z-Z)^2}, \tag{3.15}$$

and the parameters $(\mathbf{X},Z,\rho)$ describing the center and the size of the instanton in the $(\mathbf{x},z)$ space. The field strengths associated with the fields are

$$F^a_{ij} = \frac{4\rho^2}{(\xi^2+\rho^2)^2}\epsilon_{ija}, \qquad F^a_{zj} = \frac{4\rho^2}{(\xi^2+\rho^2)^2}\delta_{aj}. \tag{3.16}$$

The Chern-Simons action includes a term of the form

$$\epsilon^{MNPQ}\int \mathrm{d}^4x\mathrm{d}z\,\hat{A}_0 F^a_{MN}F^a_{PQ}, \tag{3.17}$$

and the generated electric field is

$$\hat{A}_0 = \frac{1}{8\pi^2 a}\frac{1}{\xi}\left(1 - \frac{\rho^4}{(\xi^2+\rho^2)^4}\right) + \mu, \tag{3.18}$$

where μ is an integration constant dual to the baryonic chemical potential, which we set to zero. We expand the mass equation up to order λ^{-1} thus including the effects of the curved background in the Yang-Mills action and of the Chern-Simons term: The new mass formula reads [38]

$$\begin{aligned} M &= M^{\mathrm{flat}}_{\mathrm{YM}} + \delta M_{\mathrm{YM}} + M_{\mathrm{CS}} \\ &= 8\pi^2\kappa\left[1 + \lambda^{-1}\left(\frac{\rho^2}{6} + \frac{1}{320\pi^4 a^2}\frac{1}{\rho^2} + \frac{Z^2}{3}\right)\right]. \end{aligned} \tag{3.19}$$

Minimizing this quantity leads us to the values of the size ρ,

$$\rho^2 = \frac{1}{8\pi^2 a\lambda}\sqrt{\frac{6}{5}}, \tag{3.20}$$

and the position $Z = 0$ of the classical configuration [38]. The scaling with an inverse power of λ of the instanton size justifies our expansion around flat space, since the instanton will be localized in a small region around $Z = 0$ in the large-λ limit. By plugging this result back into the mass equation, we find the classical value of the mass

$$M = 8\pi^2\kappa + N_c\sqrt{\frac{2}{15}}. \tag{3.21}$$

The near BPST limit works because at large λ the instanton is very small and thus is concentrated in a region much smaller than the radius of spacetime curvature [38,41,42]. With the calibration (3.12), the mass of the classical baryon is found to be

$$M \simeq M_{\mathrm{KK}} \times 1.684 \simeq 1598\ \mathrm{GeV}. \tag{3.22}$$

There are other $1/\lambda$ corrections and also quantum $1/N_c$ corrections to be taken into account: By quantization of the moduli space, we take into account the leading quantum corrections.

Translations and rotations in flat three-dimensional space (in the directions x^i) are exact symmetries. Translations of the solution are realized by changing the parameter $\mathbf{X}$, hence they are exact moduli. Rotations are described by an $SO(3)$ matrix R_{ij} that acts on the coordinates as

$$x^i \to R^i{}_j x^j, \tag{3.23}$$

or, alternatively, by an $SU(2)$ matrix B related to R_{ij} by

$$R_{ij} = \frac{1}{2}\mathrm{Tr}(\tau^i B \tau^j B^\dagger). \tag{3.24}$$

Rotations in flavor $SU(2)$ space are also an exact symmetry and are described by the rotations of Pauli matrices τ^i with matrices a as

$$\tau^i \to a\tau^i a^\dagger. \tag{3.25}$$

Because of the particular structure of the soliton, however, the two kinds of rotations, those in coordinate space and those in flavor space, are related (the same that happens for skyrmions), so that only one set of rotational moduli are necessary to describe all possible configurations. This will no longer be true when we turn on the mass splitting, since the isospin symmetry will be explicitly broken, so here we will use only the spatial rotations as the true moduli.

The full solution is provided in Ref. [39], and since we will only care about angular velocity terms, we will neglect the time derivatives of other moduli,

$$\begin{aligned}
A_M &= -\mathrm{i}f(\xi)V(g\partial_M g^{-1})V^{-1} - \mathrm{i}V\partial_M V^{-1},\\
A_0 &= 0,\\
\hat{A}_i &= -\frac{N_c}{16\pi^2\kappa}\frac{\rho^2}{(\xi^2+\rho^2)^2}\epsilon_{iab}\chi^a x^b,\\
\hat{A}_z &= -\frac{N_c}{16\pi^2\kappa}\frac{\rho^2}{(\xi^2+\rho^2)^2}\boldsymbol{\chi}\cdot\mathbf{x},\\
\hat{A}_0 &= \frac{N_c}{8\pi^2\kappa}\frac{1}{\xi^2}\left[1-\frac{\rho^4}{(\xi^2+\rho^2)^2}\right].
\end{aligned} \tag{3.26}$$

Inserting these fields in the action will give the moments of inertia of the soliton. We note that the angular velocity is denoted by χ^a here, as is standard in the Sakai-Sugimoto model [38] and the $SU(2)$-rotation matrix is here a, whereas in Sec. II we used the notation Ω_i [see Eq. (2.29)] for the angular velocity and $A^\dagger$ for the corresponding rotation matrix. In particular, we have

$$\chi^a = -\mathrm{i}\mathrm{Tr}(a^\dagger \dot{a}\tau^a). \tag{3.27}$$

The Lagrangian of the collective modes is, at the highest order in λ, given by the instanton moduli space dynamics lifted by the mass for the z translation and size ρ,

$$\begin{aligned}
L = &-M_0 + \frac{M_0}{2}\dot{\mathbf{X}}^2 + \frac{M_0}{2}\dot{Z}^2 - \frac{M_0\omega_Z^2}{2}Z^2\\
&+ M_0(\dot{\rho}^2 + \rho^2\dot{a}_I^2) - M_0\omega_\rho^2\rho^2 - \frac{Q}{\rho^2},
\end{aligned} \tag{3.28}$$

with

$$M_0 = 8\pi^2\kappa, \quad \omega_Z^2 = \frac{2}{3}, \quad \omega_\rho^2 = \frac{1}{6}, \quad Q = \frac{N_c}{40\pi^2 a}. \tag{3.29}$$

This is equivalent to a skyrmion with mass M_0 and diagonal moment of inertia equal to

$$I_0 = \frac{1}{2}M_0\rho^2 = \frac{1}{2}N_c\sqrt{\frac{6}{5}}, \tag{3.30}$$

with the calibration (3.12) yielding

$$I_0 \simeq \frac{1.64}{M_{\mathrm{KK}}} \simeq 1.73\ \mathrm{GeV}^{-1}. \tag{3.31}$$

Thus, including only the classical soliton energy and the rotational energy, we have

$$\begin{aligned}
M_{p,n} &= M_0 + \frac{3}{8I_0} = 0.775\ \mathrm{GeV},\\
M_\Delta &= M_0 + \frac{15}{8I_0} = 1.64\ \mathrm{GeV},\\
M_\Delta - M_{n,p} &= \frac{3}{2I_0} = 0.87\ \mathrm{GeV}.
\end{aligned} \tag{3.32}$$

This is just an estimate of the values, in fact, the BPST solution is modified at large distances, larger than $1/M_{\mathrm{KK}}$. This computation can be done since at those distances we are in the linear regime, so taking the curvature effect into account becomes simpler. The coefficient of the linear tail can be computed with the Green's function in curved space [39]. The A_z field in the singular gauge (neglecting the a moduli for the moment) reads

$$A_z^{(\mathrm{S})} = \left(\frac{1}{\xi^2} - \frac{1}{\xi^2+\rho^2}\right)\mathbf{x}\cdot\boldsymbol{\tau}, \tag{3.33}$$

which at distances larger than the soliton radius ($\xi \ll \rho$), but smaller than the curvature scale ($h(z) \simeq k(z) \simeq 1$), is approximated by

$$A_z^{(\mathrm{S})} \simeq \frac{\rho^2}{\xi^4}\mathbf{x}\cdot\boldsymbol{\tau} = -\frac{\rho^2}{2}\nabla\left(\frac{1}{\xi^2}\right)\cdot\boldsymbol{\tau}. \tag{3.34}$$

Note that $-\frac{1}{4\pi^2\xi^2}$ is the Green's function in flat four-dimensional space. To generalize to the large distance region, we substitute it with the Green's function in curved space [39]

$$H(r,0,z,0) = -\kappa \sum_{k=0}^{\infty} \phi_k(z)\phi_k(0)\frac{e^{-\sqrt{\lambda_k}r}}{4\pi r}, \tag{3.35}$$

where we already set the semiclassical value $Z = 0$; we chose $\mathbf{X} = 0$ without loss of generality and inserted the mesonic eigenmodes and eigenvalues defined as solutions of the Sturm-Liouville equation,

$$-h(z)^{-1}\partial_z(k(z)\partial_z\psi_n(z)) = \lambda_n\psi_n(z). \tag{3.36}$$

The $n = 0$ solution corresponds to a non-normalizable mode with zero mass (before taking into account the Aharony-Kutasov action), dual to the pion wave function, while the other $n > 0$ modes correspond to massive vector mesons,

$$\phi_0(z) = \frac{1}{\sqrt{\kappa\pi}}\frac{1}{k(z)}, \tag{3.37}$$

$$\phi_n(z) = \frac{1}{\sqrt{\lambda_n}}\partial_z\psi_n(z). \tag{3.38}$$

These modes (except the $n = 0$ one) can be normalized with the relations

$$\kappa\int \mathrm{d}z\, h(z)\psi_n(z)\psi_m(z) = \delta_{nm},$$
$$\kappa\int \mathrm{d}z\, k(z)\phi_n(z)\phi_m(z) = \delta_{nm}. \tag{3.39}$$

The Skyrme truncation amounts to including only the pion (and the η that shares the same mode), so that the $A_z^{(\mathrm{S})}$ field is expanded as

$$A_z^{(\mathrm{S})} \simeq -\frac{\pi}{2}\kappa\rho^2\phi_0(z)\phi_0(0)\nabla\left(\frac{1}{r}\right)\cdot\boldsymbol{\tau} + \sum_{n=1}^{\infty}\cdots. \tag{3.40}$$

In order to read off the coefficient of the three-dimensional linear tail, we need to isolate the r dependence, while integrating the pion profile in the holographic direction. Using Eq. (3.37) we obtain

$$\int_{-\infty}^{+\infty}\mathrm{d}z A_z^{(\mathrm{S})} \simeq -\pi\kappa\rho^2\frac{1}{2\kappa\pi}\int_{-\infty}^{+\infty}\mathrm{d}z\frac{1}{k(z)}\nabla\left(\frac{1}{r}\right)\cdot\boldsymbol{\tau}. \tag{3.41}$$

The integral gives a factor of π and we can use the semiclassical size $\rho^2 = \frac{N_c}{8\pi^2\kappa}\sqrt{\frac{6}{5}}$ to obtain

$$\int_{-\infty}^{+\infty}\mathrm{d}z A_z^{(\mathrm{S})} \simeq -\frac{N_c}{16\pi\kappa}\sqrt{\frac{6}{5}}\nabla\left(\frac{1}{r}\right)\cdot\boldsymbol{\tau}. \tag{3.42}$$

Defining the coefficients of the tail of the nonrotating soliton (in the standard orientation of the hedgehog) as

$$\frac{1}{2}\int \mathrm{d}z A_z^{a=1,2} = -C\partial_{1,2}\left(\frac{1}{r}\right), \tag{3.43}$$

$$\frac{1}{2}\int \mathrm{d}z A_z^{a=3} = -\frac{1}{2}(D+E)\partial_3\left(\frac{1}{r}\right), \tag{3.44}$$

$$\frac{1}{2}\int \mathrm{d}z \hat{A}_z = -\frac{1}{2}(D-E)\partial_3\left(\frac{1}{r}\right), \tag{3.45}$$

the final result is then read off of Eq. (3.42) as

$$C = D = E = \frac{N_c}{16\pi\kappa}\sqrt{\frac{6}{5}} = c_0\frac{1}{\lambda}, \tag{3.46}$$

using that $\hat{A}_z = 0$ for the nonrotating soliton. The coefficient c_0 is thus

$$c_0 = \frac{1}{16\pi a}\sqrt{\frac{6}{5}} = \frac{27\pi^2}{2}\sqrt{\frac{6}{5}}. \tag{3.47}$$

This is exact in the large-λ limit. To compare it with the coefficient found for the skyrmion, we need to recall that we are using different units in the two computations; here we adopted dimensionless units, meaning that dimensionful quantities need to have factors of M_{KK} restored. The integral of the gauge field is dimensionless, so the coefficient C must have the dimension of M_{KK}^{-2} to cancel that of $\nabla\frac{1}{r}$,

$$C^{\mathrm{dim}} = CM_{\mathrm{KK}}^{-2} = \frac{27\pi^2}{2M_{\mathrm{KK}}^2\lambda}\sqrt{\frac{6}{5}}$$
$$= 9.75\times10^{-6}\ \mathrm{MeV}^{-2} = (0.61\ \mathrm{fm})^2. \tag{3.48}$$

The introduction of explicit breaking of isospin symmetry within the holographic model of Sakai-Sugimoto is realized by changing the mass matrix in Eq. (3.8) to something not proportional to the identity matrix, resulting in the moment of inertia being modified, taking the form of Eq. (2.67).

Let us consider the baryon masses at $\epsilon = 0$ and how they are affected by the quark mass. Various effects have been considered in the past, e.g., the leading-order effect for $\epsilon = 0$ and a finite quark mass is a shift in the meson and baryon spectra in both the two-flavor [43] and three-flavor [44] cases. Here, we will add also the modification to the inertia which, in turn, affects the nucleon-Δ splitting. The formula (2.67) unfortunately cannot yet be used reliably at this stage to compute the mass correction to the inertia I.

The point is that we know I_0 from the self-dual instanton approximation, and we know that it receives, even at $m=0$, order $1/\lambda$ corrections from the curvature effects. The mass corrections are of the same order $\kappa C^2 \propto 1/\lambda$. So to make use of Eq. (2.67), we should first find a technique to compute also I up to order $1/\lambda$.

However, the splitting term δ can be computed within the approximation of small m: This is possible because the dominant contribution to δ in this limit comes from the soliton tails, which can be computed exactly. The linearized tail is a reliable approximation from a certain cutoff $r=R_{\mathrm{UV}}$ up to $r\to\infty$: From the WSS model we know that the cutoff should be roughly the order of the soliton size $R_{\mathrm{UV}}\sim\rho$. As we will see, and as has happened in the skyrmion case, employing the tail to compute the moment of inertia will lead to a divergent result, a hint that the correct configuration for $r<R_{\mathrm{UV}}$ is not given by the linearized tail, but by some perturbation of the BPST instanton. However, the divergent term is independent of m, while the leading order in m is linear: This linear term does not depend on R_{UV}, allowing us to compute the splitting explicitly. Performing the full numerical solution is more challenging as compared to the Skyrme model, due to the presence of the additional holographic coordinate. On the other hand in the WSS model we have an analytic approximation in the BPST instanton for the core configuration and a semianalytical expression as an expansion over mesonic modes for the linearized tail: We now move to compute the deformation of the tail induced by the presence of S_{AK}.

As a first step, we write the linearized equations of motion: Only the fields $\hat{A}_z$ and $A_z^{a=3}$ will take part in the splitting, hence we have

$$\kappa k(z)\left(\partial_i^2\hat{A}_z-\partial_i\partial_z\hat{A}_i\right)=m_q c\left[\int_{-\infty}^{+\infty}\mathrm{d}z\,\hat{A}_z+\epsilon\int_{-\infty}^{+\infty}\mathrm{d}z\,A_z^{a=3}\right],\tag{3.49}$$

$$\kappa k(z)\left(\partial_i^2A_z^{a=3}-\partial_i\partial_zA_i^{a=3}\right)=m_q c\left[\int_{-\infty}^{+\infty}\mathrm{d}z\,A_z^{a=3}+\epsilon\int_{-\infty}^{+\infty}\mathrm{d}z\,\hat{A}_z\right].\tag{3.50}$$

We immediately see that the equations are coupled: This is a consequence of the mass matrix of the pions (and η) becoming nondiagonal. It is simple to diagonalize the mass matrix or, analogously, to diagonalize these two equations. To do so we introduce the mass eigenstates

$$A_\eta=\frac{1}{\sqrt{2}}(A_z^{a=3}+\hat{A}_z),\quad A_\pi=\frac{1}{\sqrt{2}}(A_z^{a=3}-\hat{A}_z).\tag{3.51}$$

We can, in principle, perform the change of basis for the fields also for the spatial components A_i, but it is not necessary: The Aharony-Kutasov action, in fact, introduces effective mass terms only for the pseudoscalar degrees of freedom, as can be easily understood once we expand the field A_z in mesonic modes. Then the holonomy of the field A_z can be written as

$$\int_{-\infty}^{+\infty}\mathrm{d}z\,A_z=\sum_{n=0}^{\infty}\varphi_n(x)\int_{-\infty}^{+\infty}\mathrm{d}z\,\phi_n(z)=\phi_0(x)\pi+\sum_{n=1}^{\infty}\varphi_n(x)\int_{-\infty}^{+\infty}\mathrm{d}z\,\partial_z\psi_n(z),\tag{3.52}$$

and since the functions $\psi_n(z)$ vanish at the UV boundary, only the first term in the sum survives, generating a mass term for the pseudoscalars. Because of this, we will restrict our analysis to the z component of the fields: After diagonalization, it is easy to read the mass eigenvalues as being

$$m_\pm^2=m^2(1\pm\epsilon),\tag{3.53}$$

so we can make an educated guess for the shape of the solution: The asymptotic configuration in the massless scenario is given by

$$\hat{A}_z\simeq\frac{\rho^2N_c}{8\kappa}\chi^j\partial_{X^j}H(\mathbf{x},\mathbf{X},z,Z),\tag{3.54}$$

$$A_z^{a=3}\simeq-2\pi^2\rho^2\mathrm{Tr}(a\tau^ka^\dagger\tau^3)\partial_{X^k}H(\mathbf{x},\mathbf{X},z,Z),\tag{3.55}$$

with

$$H(\mathbf{x},\mathbf{X},z,Z)=\kappa\sum_{n=0}^{\infty}\phi_n(z)\phi_n(Z)Y_n(r),\qquad Y_n(r)=-\frac{1}{4\pi}\frac{e^{-\sqrt{\lambda_n}r}}{r},\tag{3.56}$$

and we can easily think of keeping this general shape, while providing a nonvanishing λ_0 to account for the pion mass. However, we have a mass splitting here, so we need to introduce two values $\lambda_\pm=m^2(1\pm\epsilon)$. Moreover, the mass eigenstates are combinations of the fields (3.54) and (3.55), so we build an *Ansatz* for A_η, A_π given by

$$A_\eta=b\chi^j\partial_{X^j}H_+-\tilde{b}\mathrm{Tr}(a\tau^ja^\dagger\tau^3)\partial_{X^j}H_+,\tag{3.57}$$

$$A_\pi=d\chi^j\partial_{X^j}H_--\tilde{d}\mathrm{Tr}(a\tau^ja^\dagger\tau^3)\partial_{X^j}H_-.\tag{3.58}$$

The constants should be determined by the boundary conditions (the matching with the core configuration in an intermediate region), while the functions $H_\pm$ are given by

$$H_\pm\equiv-\kappa\sum_{n=0}\phi_n(z)\phi_n(Z)\frac{1}{4\pi}\frac{e^{-\sqrt{\lambda_n}r}}{r},\quad\lambda_0=m_\pm^2.\tag{3.59}$$

With this choice, the equations of motion are satisfied, and we only need to fix the constants: We then require that in the massless limit the fields revert to

$$\lim_{m\to 0} A_\eta = \hat{A}_z, \qquad \lim_{m\to 0} A_\pi = A_z^{a=3}, \tag{3.60}$$

and we obtain

$$b = -d, \qquad \tilde{b} = \tilde{d}. \tag{3.61}$$

To conclude, we also require matching with the core of the baryon solution, which is equivalent to requiring that the coefficients of Eqs. (3.54) and (3.55) are reproduced. This fixes all the constants as

$$b = \frac{\rho^2 N_c}{\sqrt{2}8\kappa}, \qquad \tilde{b} = \sqrt{2}\pi^2\rho^2 = C = D = E. \tag{3.62}$$

Now that the solution is fixed, we note that since only the neutral pion and η masses are modified, we can neglect the vector mesons in the computation of the splitting: They will contribute to the total moment of inertia, but with a term proportional to the identity matrix. To isolate the pseudoscalars, we remove them from the sum in the functions $H_\pm$ and define new Yukawa potentials $Y_\pm(r)$,

$$H_\pm = \kappa\phi_0(z)\phi_0(Z)Y_\pm(r) + \kappa\sum_{n=1}^{\infty}\phi_n(z)\phi_n(Z)Y_n(r),$$
$$Y_\pm(r) = -\frac{1}{4\pi}\frac{e^{-m_\pm r}}{r}. \tag{3.63}$$

We can read off the inertia tensor from the terms in the Lagrangian that are quadratic in the angular velocity $\boldsymbol{\chi}$: Such contributions can arise from all terms of the action, the Yang-Mills, Chern-Simons, and Aharony-Kutasov parts. The leading contribution to the inertia splitting is given in the small-m limit by a linear term, hence we discard corrections coming from the Aharony-Kutasov term, whose prefactor is of order $m_q c \sim m^2 f_\pi^2$. Moreover, the leading contribution comes from the linearized soliton tail, hence we neglect the Chern-Simons term, being at least cubic in the fields. We are then left with the Yang-Mills action to be computed on the solution of the equations of motion just obtained. The action terms we are looking for are the ones involving the $\mathcal{A}_z$ and at most quadratic in the fields

$$S_{\rm YM}|_{\mathcal{A}_z} = -\kappa{\rm Tr}\int {\rm d}^4x{\rm d}z\, k(z)[(\partial_i\mathcal{A}_z)^2 - (\partial_0\mathcal{A}_z)^2], \tag{3.64}$$

which receives contributions both from the $A_z^{a=1,2}$ and the A_η, A_π fields, which we split into two terms, defining the kinetic energy parts as

$$\begin{aligned} T^{(1,2)} &= \frac{\kappa}{2}\sum_{a=1}^{2}\int {\rm d}z{\rm d}^3x\, k(z)\left[(\partial_i A_z^a)^2 - (\partial_0 A_z^a)^2\right], \\ T^{(3)} &= \frac{\kappa}{2}\int {\rm d}z{\rm d}^3x\, k(z)\left[(\partial_i A_z^3)^2 - (\partial_0 A_z^3)^2 + (\partial_i\hat{A}_z)^2 - (\partial_0\hat{A}_z)^2\right] \\ &= \frac{\kappa}{2}\int {\rm d}z{\rm d}^3x\, k(z)\left[(\partial_i A_\eta)^2 - (\partial_0 A_\eta)^2 + (\partial_i A_\pi)^2 - (\partial_0 A_\pi)^2\right], \end{aligned} \tag{3.65}$$

where we have used Eq. (3.1) and the total kinetic energy is $T = T^{(1,2)} + T^{(3)}$. Starting from the latter, which gives rise to the following terms at order χ^2,

$$\begin{aligned} &{\rm Tr}\int {\rm d}z{\rm d}^3x\, k(z)\left[(\partial_i A_\eta)^2 + (\partial_i A_\pi)^2\right] \\ &= b^2\chi^j\chi^k\int {\rm d}^3x{\rm d}z\, k(z)(\partial_i\partial_j H_+\partial_i\partial_k H_+ + \partial_i\partial_j H_-\partial_i\partial_k H_-), \end{aligned} \tag{3.66}$$

$$\begin{aligned} &-{\rm Tr}\int {\rm d}z{\rm d}^3x\, k(z)\left[(\partial_0 A_\eta)^2 + (\partial_0 A_\pi)^2\right] \\ &= -4\tilde{b}^2\dot{R}_{a3}\dot{R}_{k3}\int {\rm d}^3x{\rm d}z\, k(z)(\partial_a H_+\partial_k H_+ + \partial_a H_-\partial_k H_-). \end{aligned} \tag{3.67}$$

We see immediately that the terms in Eq. (3.66) produce kinetic energy contributions proportional to the identity matrix, since after integrating over the angular coordinates of $\mathbb{R}^3$ we are left with something proportional to $\boldsymbol{\chi}\cdot\boldsymbol{\chi}$. On the other hand, the terms in Eq. (3.67) do break spherical symmetry, since they select the direction in coordinate space that corresponds to the rotation performed by R_{a3}, that is, the direction that we obtain for the orientation of π^3 after the moduli a are applied to the soliton configuration. With the standard hedgehog orientation, this direction would simply be given by $\hat{x}^3$. We then introduce the body-fixed axis and give the components of the angular velocity in terms of this coordinate system: We label them $(\chi_\xi, \chi_\eta, \chi_\zeta)$, where χ_ζ identifies the projection along the axis of residual symmetry (again, in the case of standard orientation, $\chi_\zeta = \chi_3$). This leads us to consider only the terms in Eq. (3.67), which can then be computed by using the relations

$$\dot{R}_{ab} = \epsilon_{amn}\chi_m R_{nb}, \tag{3.68}$$

$$\int \mathrm{d}^3x\, \partial_i f(r)\partial_j f(r) = \frac{4\pi}{3}\delta_{ij}\int \mathrm{d}r\, r^2 f'(r)^2, \tag{3.69}$$

$$\begin{aligned}\epsilon^{akb}\epsilon^{acd}\chi^k\chi^c R_{b3}R_{d3} &= \chi^2 R_{b3}R_{b3} - (\chi^a R_{a3}\chi^b R_{b3}) \\ &= \chi^2 - \chi_\zeta^2,\end{aligned} \tag{3.70}$$

$$\begin{aligned}\int_R^\infty \mathrm{d}r \frac{(m_\pm r+1)^2}{r^2} e^{-2m_\pm r} &= \left(\frac{m_\pm}{2}+\frac{1}{R}\right)e^{-2m_\pm R} \\ &\simeq \frac{1}{R} - \frac{3}{2}m_\pm + \mathcal{O}(m^2).\end{aligned} \tag{3.71}$$

After keeping only the $n = 0$ term in the mesonic modes' expansion of the fields (higher n does not contribute to the splitting, while cross terms vanish because of orthogonality relations), we can write the following kinetic energy term $T^{(3)}$ for the fields A_η, A_π:[2]

$$T^{(3)} = \frac{1}{3}\pi^2\kappa\rho^4(\chi^2 - \chi_\zeta^2)\left[\frac{2}{R} - \frac{3}{2}(m_+ + m_-)\right] + \mathcal{O}(m^2). \tag{3.72}$$

This formula presents a UV divergent term proportional to R^{-1}, with R being a cutoff to the integral over r, which arises from the extrapolation of the linear tail to the core region. Realistically, the cutoff R is not to be sent to zero, but rather to some value of the order of the soliton size ρ. In this way, we can provide an estimate on the order of this term, however, it is not necessary since we can argue that it cannot contribute to the splitting: In fact, this term is independent of the parameters m, ϵ, so we cannot regard it as a correction to the inertia due to the presence of the Aharony-Kutasov term. It is instead to be interpreted as the correction to the inertia due to the deviation of the tail of the soliton from the BPST instanton configuration, ultimately due to the curved background.

The last part we need to compute is the contribution to the inertia of the fields $A_z^{a=1,2}$: The computation is analogous to the one performed above, with the only exception being that every instance of $m_\pm$ is substituted with m, and formula (3.70) has to be modified in favor of the components χ_ξ, χ_η. The resulting contribution is then given by

$$T^{(1,2)} = \frac{2}{3}\pi^2\kappa\rho^4(\chi^2 + \chi_\zeta^2)\left[\frac{1}{R} - \frac{3}{2}m\right] + \mathcal{O}(m^2). \tag{3.73}$$

The sum of the two terms finally gives the complete rotational kinetic energy $T = T^{(1,2)} + T^{(3)}$,

$$\begin{aligned}T = \frac{\pi^2\rho^4\kappa}{2}m\Bigg[&\left(\frac{8}{3mR} - \left(2+\sqrt{1+\epsilon}+\sqrt{1-\epsilon}\right)\right)\chi^2 \\ &- \left(2-\sqrt{1+\epsilon}-\sqrt{1-\epsilon}\right)\chi_\zeta^2\Bigg].\end{aligned} \tag{3.74}$$

We thus confirm that the UV divergent term does not enter in the splitting, and we can see by expanding the square roots that the splitting term δ appears at order $m\epsilon^2$. We can then compute the splitting δ of Eq. (2.67),

$$\delta = \frac{\pi^2\rho^4\kappa}{12}m\epsilon^2 + \mathcal{O}(m^2, \epsilon^4). \tag{3.75}$$

A. New quantization for $\epsilon \neq 0$ and Δ splitting

In this section, we derive a quantum mechanical Hamiltonian for the baryon spectrum up to order ϵ^2. To do so, we take into account two main effects: One is the perturbation of the moment of inertia due to the presence of the quark mass term, which we already analyzed in the small-m limit, while the second is the presence of a term linear in the angular velocity in the action, arising from the Aharony-Kutasov action evaluated on the unperturbed baryon configuration. [It arises, in general, on the full configuration, and we can see the presence of linear terms already in the previous section, arising from cross terms proportional to $b\tilde{b}$ or $d\tilde{d}$ [see Eq. (3.61) and the *Ansätze* (3.57) and (3.58)], but they are subleading contributions in m when compared to the ones arising from the unperturbed baryon core.]

We have already computed the new moments of inertia of the soliton, so the kinetic part of the Lagrangian coming from the Yang-Mills action, neglecting the motion of the center of mass, reads

$$L_{\mathrm{YM}} = \frac{1}{2}I_A(\chi_\xi^2 + \chi_\eta^2) + \frac{1}{2}I_C\chi_\zeta^2 - M, \tag{3.76}$$

where

$$I_A = I + \delta, \qquad I_C = I - 2\delta. \tag{3.77}$$

Again, we have relaxed the choice of a frame in which the axis of the cylindrical symmetry is oriented along $\hat{x}^3$: We decomposed the angular velocity in components along principal axes of inertia of this "rigid top," while the spatial orientation of these axes is completely free.

If this was the complete Lagrangian, it would be straightforward to get the Hamiltonian: We simply need to trade angular velocities for their conjugate momenta $J_j = \mathcal{I}_{jk}\chi_k$ to obtain the Hamiltonian of a rigid symmetrical top as in Eq. (2.80),

$$E_{\mathrm{top}} = \frac{1}{2I_A}j(j+1) + \frac{1}{2}\left(\frac{1}{I_C} - \frac{1}{I_A}\right)j_3^2 + M. \tag{3.78}$$

However, it would be naive to extract the Hamiltonian by simply identifying $J_j = \mathcal{I}_{jk}\chi_k$: The Aharony-Kutasov

[2]The mass shift induced on the configuration by including the quark mass for $\epsilon = 0$ [43,44] is an order m^2 effect and alters only the potential energy.

action provides a Lagrangian term linear in the angular velocity. This term arises at the first order in perturbation theory, hence it is obtained by feeding the unperturbed baryon configuration to the perturbation Lagrangian, in this case provided by the Aharony-Kutasov term (3.8). As noted before, at the static order ($\boldsymbol{\chi} = 0$) the terms proportional to ϵ vanish due to the trace: The first nonvanishing $\mathcal{O}(\epsilon)$ term arises at linear order in χ, hence it is an N_c^{-1} correction to the baryon mass. To show the mechanism as presented in Ref. [31], we start with the Aharony-Kutasov Lagrangian written in terms of U, φ as defined in Eq. (3.7),

$$L_{\mathrm{AK}} = c\mathrm{Tr}\int \mathrm{d}^3x[Me^{\mathrm{i}\varphi}aUa^\dagger + e^{-\mathrm{i}\varphi}aU^\dagger a^\dagger M - 2\mathbb{1}_2]. \tag{3.79}$$

We then write the matrix U using the BPST instanton approximation,

$$U = -\cos\alpha + \mathrm{i}\sin\alpha\hat{\mathbf{x}}\cdot\boldsymbol{\tau}, \qquad \alpha = \frac{\pi}{\sqrt{1+\frac{\rho^2}{r^2}}}, \tag{3.80}$$

where the function $\alpha(r)$ is defined by the integral over z of the field A_z in the unperturbed baryon configuration. We can then keep the terms proportional to ϵ and expand the exponential to linear order in φ,

$$\begin{aligned} L^{\epsilon}_{\mathrm{AK}} &= 2m_q c\epsilon\int \mathrm{d}^3x\,\varphi\sin\alpha\frac{x^i}{r}\mathrm{Tr}[\tau^3 a\tau^i a^\dagger] \\ &= \frac{m_q c\epsilon N_c}{16\pi\kappa}\int \mathrm{d}^3x\,\sin\alpha\frac{1}{\rho\left(1+\frac{r^2}{\rho^2}\right)^{\frac{3}{2}}}\frac{x^i x^j}{r}R_{3i}\chi^j \\ &= \frac{m_q c\epsilon N_c}{12\kappa}\rho^3\mathcal{J}_2\chi^i R_{3i}, \end{aligned} \tag{3.81}$$

where we made use of the $\hat{A}_z$ field as in Eq. (3.26) and we defined the integral

$$\mathcal{J}_2 \equiv \int_0^\infty \mathrm{d}y\frac{y^3}{(1+y^2)^{\frac{3}{2}}}\sin\left(\frac{\pi}{\sqrt{1+y^{-2}}}\right) \simeq 1.054. \tag{3.82}$$

The term $L^{\epsilon}_{\mathrm{AK}}$ modifies the canonical relation between angular velocity and the angular momentum, which is now given by

$$\begin{aligned} J_i &= \mathcal{I}_{ij}\chi_j + \frac{\epsilon m_q c N_c}{12\kappa}\rho^3 R_{3i}\mathcal{J}_2 \\ &= \mathcal{I}_{ij}\chi_j + \frac{\epsilon m^2 N_c}{12\pi}\rho^3 R_{3i}\mathcal{J}_2 \\ &\equiv \mathcal{I}_{ij}\chi_j - K_i. \end{aligned} \tag{3.83}$$

Notice that in the definition of K_i there appears the rotation matrix R_{3i}. This means that the vector K_i always points in the direction labeled by ζ (that is, the direction that in the body-fixed frame becomes $\hat{x}_3$). This implies that only the relation between J_ζ and χ_ζ is modified, and the full Hamiltonian is thus given by

$$\begin{aligned} H_{\mathrm{full}} &= \frac{1}{2I_A}(J_\xi^2 + J_\eta^2) + \frac{1}{2I_C}(J_\zeta^2 + K_\zeta^2 + 2J_\zeta K_\zeta) + M_0 \\ &= \frac{1}{2I_A}J^2 + \frac{1}{2}\left(\frac{1}{I_C} - \frac{1}{I_A}\right)J_\zeta^2 + \frac{1}{I_C}J_\zeta K_\zeta + \frac{1}{2I_C}K_\zeta^2 + M, \end{aligned} \tag{3.84}$$

where we have defined $K_\zeta \equiv -\frac{\epsilon m_q c N_c}{12\kappa}\rho^3\mathcal{J}_2$. We see that the Hamiltonian is still diagonal and the energies are simply obtained as

$$\begin{aligned} E_{\mathrm{full}} &= \frac{1}{2I_A}j(j+1) + \frac{1}{2}\left(\frac{1}{I_C} - \frac{1}{I_A}\right)j_3^2 + \frac{1}{I_C}K_\zeta j_3 \\ &\quad + \frac{1}{2I_C}K_\zeta^2 + M. \end{aligned} \tag{3.85}$$

We may then use the relation $J^i R_{ki} = -I^k$ to identify $J_\zeta \equiv -I_3$ so that the quantum number j_3 can be replaced by $-i_3$. We also note that the corrections ΔI are of order ϵ^2, while K_ζ is of order ϵ: If we stop our analysis at order ϵ^2 we can safely replace I_C with the unperturbed I_0 in the terms proportional to K_ζ, leading to

$$\begin{aligned} E_{\mathrm{full}} &= \frac{1}{2I_A}j(j+1) + \frac{1}{2}\left(\frac{1}{I_C} - \frac{1}{I_A}\right)i_3^2 \\ &\quad - \frac{1}{I_0}K_\zeta i_3 + \frac{1}{2I_0}K_\zeta^2 + M. \end{aligned} \tag{3.86}$$

We observe two new terms in the energy formula with respect to Eq. (3.78). $\frac{1}{2I_0}K_\zeta^2$ is simply a mass shift due to the quark mass difference: We see that it is always positive and of order $\epsilon^2 m$. $-\frac{1}{I_0}K_\zeta i_3$ is the isospin breaking term that is responsible for the splitting of states with the same absolute value of i_3, i.e., the term computed in Ref. [31] that accounts for the proton-neutron mass difference. It also removes half of the degeneracy in the Δ multiplet. It is of order ϵm^2.

We immediately see that there are two contributions to the splitting of the Δ multiplet: Terms of order ϵ (giving higher mass to lower values of i_3) and terms of order ϵ^2 (not depending on the sign of isospin, but on the absolute value). This is exactly what is suggested by the separation geometry model (see Ref. [45]). The estimate we obtained for the splitting of the moment of inertia is consistent only in the $m \ll |\epsilon|$ limit: We need to keep this in mind, as we have to sum terms of order $m\epsilon^2$ (from δ) and terms of order $m^2\epsilon$ (from K_ζ). Then we consider the leading-order term in the splitting to be of order $m\epsilon^2$, which gives

$$\frac{1}{2}(M_{\Delta^{++}}-M_{\Delta^{+}}-M_{\Delta^{0}}+M_{\Delta^{-}})=\frac{3}{2}\frac{\delta}{(I+\delta)(I-2\delta)}2\simeq\frac{3\delta}{I_0^2}. \tag{3.87}$$

Assuming the previous results we get

$$\frac{1}{2}(M_{\Delta^{++}}-M_{\Delta^{+}}-M_{\Delta^{0}}+M_{\Delta^{-}})\simeq\frac{\pi^2\rho^4\kappa}{4I_0^2}m\epsilon^2\simeq\frac{27\pi}{8}\frac{m\epsilon^2}{N_c\lambda}. \tag{3.88}$$

For the numerical values we obtain

$$\frac{1}{2}(M_{\Delta^{++}}-M_{\Delta^{+}}-M_{\Delta^{0}}+M_{\Delta^{-}})\simeq 3.41\ \text{MeV}. \tag{3.89}$$

The splitting of order ϵm^2, which splits even proton and neutron masses, is instead given by

$$M_p-M_n=\frac{\epsilon m^2 N_c}{48\pi^3\kappa}\rho\mathcal{J}_2\simeq -4.74\ \text{MeV}. \tag{3.90}$$

A dimensionless quantity we can compute is the ratio of the splitting with the semiclassical nucleon mass [46]

$$\begin{aligned}\frac{M_p-M_n}{M_N}&=-1.78\times10^{-3},\\ \left[\frac{M_p-M_n}{M_N}\right]_{\text{exp}}&=-1.38\times10^{-3},\end{aligned} \tag{3.91}$$

where we have used the quantum-corrected approximate mass [38],

$$M(\ell)=8\pi^2\kappa+\sqrt{\frac{(\ell+1)^2}{6}+\frac{2N_c^2}{15}}+\frac{2}{\sqrt{6}}, \tag{3.92}$$

with the nucleon mass $M_N=M(1)$. The full pattern of splittings in the Δ multiplet is then obtained by combining these two contributions,

$$\begin{aligned}M_{\Delta^{++}}-M_{\Delta^{+}}&=\frac{3\delta}{I_0^2}+\frac{\epsilon m^2 N_c}{48\pi^3\kappa}\rho\mathcal{J}_2=-1.25\ \text{MeV},\\ M_{\Delta^{+}}-M_{\Delta^{0}}&=\frac{\epsilon m^2 N_c}{48\pi^3\kappa}\rho\mathcal{J}_2=-4.67\ \text{MeV},\\ M_{\Delta^{0}}-M_{\Delta^{-}}&=-\frac{3\delta}{I_0^2}+\frac{\epsilon m^2 N_c}{48\pi^3\kappa}\rho\mathcal{J}_2=-8.08\ \text{MeV}.\end{aligned} \tag{3.93}$$

The ratio of the splitting with the semiclassical Δ mass is

$$\begin{aligned}\frac{M_{\Delta^{++}}-M_{\Delta^{+}}}{M_\Delta}&=-3.92\times10^{-4},\\ \frac{M_{\Delta^{+}}-M_{\Delta^{0}}}{M_\Delta}&=-1.46\times10^{-3},\\ \frac{M_{\Delta^{0}}-M_{\Delta^{-}}}{M_\Delta}&=-2.53\times10^{-3},\end{aligned} \tag{3.94}$$

with the Δ mass $M_\Delta=M(3)$ of Eq. (3.92). The mass splitting is illustrated in Fig. 12, where we show the two consecutive splittings with different colors. The first splitting shown with blue dashed lines is due to the splitting that

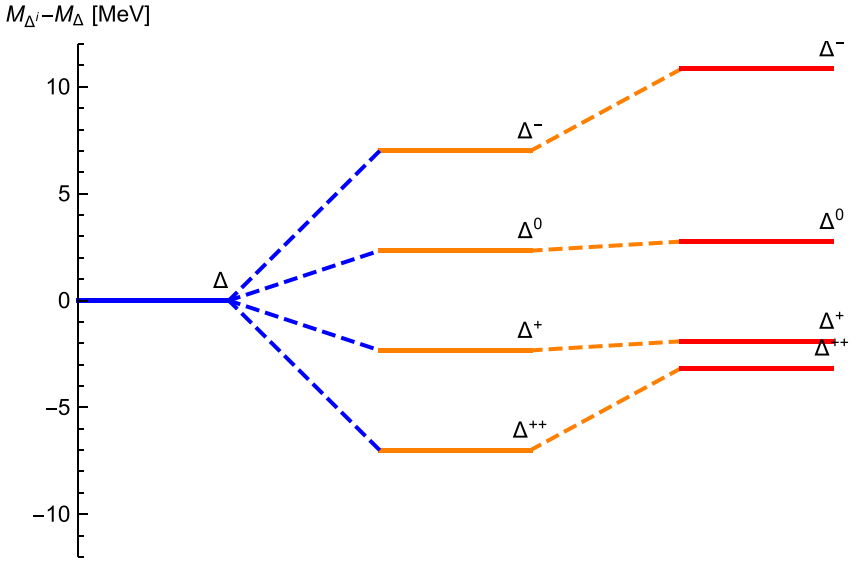

FIG. 12. The mass spectrum of the Δ multiplet, measured with respect to the semiclassical mass. The first splitting (from left) shown with blue dashed lines is due to the splitting that is linear in the isospin quantum number j_3, but quadratic in the pion mass m, corresponding to the result of Ref. [31]. The orange dashed correction shown subsequently is our result that is quadratic in j_3, but linear in m.

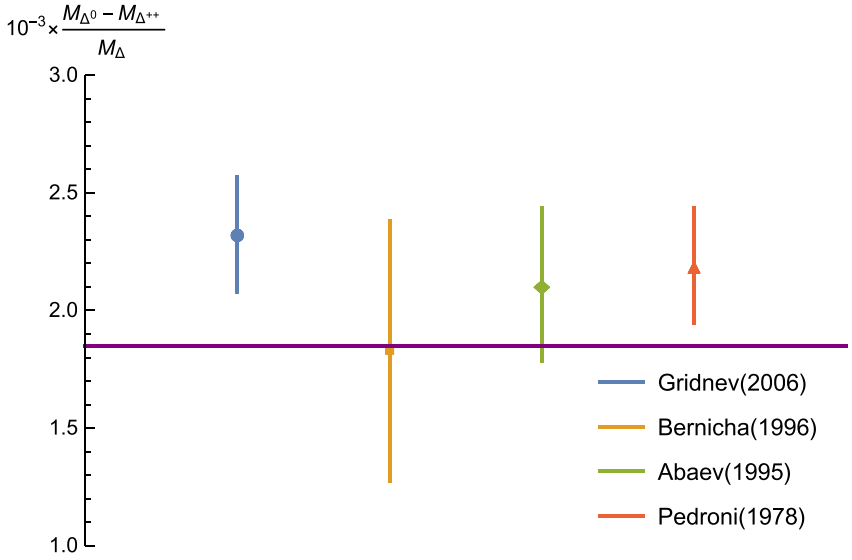

FIG. 13. The mass splitting between the Δ^{++} state and the Δ^0 state, which is measured experimentally by different groups: Pedroni [47], Abaev and Kruglov [48], Bernicha *et al.* [49], and Gridnev *et al.* [50]. Our result is shown with the purple horizontal line.

is linear in the isospin quantum number j_3, but quadratic in the pion mass m, corresponding to the result of Ref. [31]. The orange dashed correction shown to the right is our result of the splitting that is quadratic in j_3, but linear in m. Notice that our splitting contribution does not distinguish the sign of the isospin quantum number, but only the magnitude. It therefore only shifts the neutron-proton masses upward without contributing to the neutron-proton mass difference. The sum of the first two splittings in Eq. (3.94) is measured experimentally [47–50] and compared with our result in Fig. 13.

IV. CONCLUSION AND DISCUSSION

We summarize the main novel aspects presented in this paper:

(i) We have developed a technique to study the first-order contribution to the moments of inertia due to the mass term. This term is due to the linear tail effect and is linear in the pion mass.

(ii) We used this technique to compute the deviation of the inertia tensor of the skyrmion, also in the presence of isospin breaking due to the quark mass difference. In this case, we could also perform the numerical computation for all values of the mass, and we confirmed that the technique works well when the mass is small. This allows us to compute a partial splitting in the baryon states, for example, in the Δ spectrum, but it is not able to split the neutron-proton masses.

(iii) We then performed the computation of the splitting of the moments of inertia in the WSS model of holographic QCD. Here we cannot perform the numerical computation due to the complexity of the problem, but we can apply our technique in the small-mass limit.

(iv) In the WSS model, there is also another source of splitting of baryon masses due to the presence of vector mesons and the Chern-Simons term [31] (this mass splitting mechanism is similar to that of Ref. [25] in the context of the Skyrme model with η, ω, and ρ mesons). Here we can thus see the combination of these effects, with the one we derived splitting the moments of inertia. This allowed us to complete the spectrum of the Δ multiplet with no unwanted degeneracy and no equidistant splitting between the states.

We computed the mass splitting of the Δ's in the Skyrme and WSS models, in the case of two quark flavors and in the large-N_c limit, hence it is safe to neglect the η mass coming from the axial anomaly. We are aware that for a more realistic prediction we would need to include the anomaly term and also add the strange quark with its corresponding mass. Such an extension to a more physically relevant analysis is left for future work.

It would be interesting to use our result in more complex cases, for example, for multiskyrmion states, but we leave such a study for the future.

In the case of the Skyrme model, it was possible to perform a full numerical computation of the moments of inertia for any value of the pion/quark mass. This enabled us to confirm the leading-order results in the pion mass for both the moment of inertia and for the splitting of the Δ's. The corresponding full numerical computation in the WSS model would be much harder to carry out and thus we limit our analysis to the first-order approximation linear in the pion mass.

The final result in the WSS model is a hierarchy of masses for the Δ multiplet $M_{\Delta^{++}} < M_{\Delta^{+}} < M_{\Delta^{0}} < M_{\Delta^{-}}$ and a hierarchy of splittings $M_{\Delta^{+}} - M_{\Delta^{++}} < M_{\Delta^{0}} - M_{\Delta^{+}} < M_{\Delta^{-}} - M_{\Delta^{0}}$. Clearly this is valid only in the limits considered, i.e., large-N_c, large-λ, and small m, extrapolated to the calibrated parameters. We want to point out that the final result is very sensitive to details. The very fact that the skyrmion is prolate and not oblate may change once the η mass coming from the axial anomaly is considered or when the full numerical computation is done. Moreover, the precise hierarchy of masses is also very dependent on the precise relation between the splittings (3.90) and (3.87), which happen to be very similar in magnitude.

ACKNOWLEDGMENTS

The work of L. B. is supported by the National Natural Science Foundation of China (Grant No. 12150410316). The work of S. B. is supported by the INFN special research project grant "GAST" (gauge and string theories). S. B. G. thanks the Outstanding Talent Program of Henan University and the Ministry of Education of Henan Province for partial support. The work of S. B. G. is supported by the National Natural Science Foundation of China (Grants No. 11675223 and No. 12071111) and by the Ministry of Science and Technology of China (Grant No. G2022026021L).

[1] T. H. R. Skyrme, A nonlinear field theory, Proc. R. Soc. A **260**, 127 (1961).
[2] T. H. R. Skyrme, A unified field theory of mesons and baryons, Nucl. Phys. **31**, 556 (1962).
[3] I. Zahed and G. E. Brown, The Skyrme model, Phys. Rep. **142**, 1 (1986).
[4] Y.-L. Ma and M. Harada, Lecture notes on the Skyrme model, arXiv:1604.04850.
[5] G. S. Adkins, C. R. Nappi, and E. Witten, Static properties of nucleons in the Skyrme model, Nucl. Phys. **B228**, 552 (1983).
[6] P. Simic, QCD at large N_c: Skyrme or the bag?, Phys. Rev. Lett. **55**, 40 (1985).
[7] G. S. Adkins and C. R. Nappi, The Skyrme model with pion masses, Nucl. Phys. **B233**, 109 (1984).
[8] R. Battye and P. Sutcliffe, Skyrmions and the pion mass, Nucl. Phys. **B705**, 384 (2005).
[9] R. Battye and P. Sutcliffe, Skyrmions with massive pions, Phys. Rev. C **73**, 055205 (2006).
[10] C. Houghton and S. Magee, The effect of pion mass on Skyrme configurations, Europhys. Lett. **77**, 11001 (2007).
[11] R. Battye, N. S. Manton, and P. Sutcliffe, Skyrmions and the alpha-particle model of nuclei, Proc. R. Soc. A **463**, 261 (2007).
[12] T. Fujiwara, Y. Igarashi, A. Kobayashi, H. Otsu, T. Sato, and S. Sawada, An effective Lagrangian for pions, ρ mesons and skyrmions, Prog. Theor. Phys. **74**, 128 (1985).
[13] U. G. Meissner, N. Kaiser, H. Weigel, and J. Schechter, Realistic pseudoscalar—vector Lagrangian. 2. Static and dynamical baryon properties, Phys. Rev. D **39**, 1956 (1989); **40**, 262(E) (1989).
[14] U. G. Meissner, N. Kaiser, A. Wirzba, and W. Weise, Skyrmions with ρ and ω mesons as dynamical gauge bosons, Phys. Rev. Lett. **57**, 1676 (1986).
[15] P. Jain, R. Johnson, U. G. Meissner, N. W. Park, and J. Schechter, Realistic pseudoscalar vector chiral Lagrangian and its soliton excitations, Phys. Rev. D **37**, 3252 (1988).
[16] J. Schechter and H. Weigel, The Skyrme model for baryons, arXiv:hep-ph/9907554.
[17] O. Kaymakcalan and J. Schechter, Chiral Lagrangian of pseudoscalars and vectors, Phys. Rev. D **31**, 1109 (1985).
[18] C. Naya and P. Sutcliffe, Skyrmions in models with pions and rho mesons, J. High Energy Phys. 05 (2018) 174.
[19] C. Naya and P. Sutcliffe, Skyrmions and clustering in light nuclei, Phys. Rev. Lett. **121**, 232002 (2018).
[20] E. Witten, Baryons in the 1/n expansion, Nucl. Phys. **B160**, 57 (1979).
[21] M. Durgut and N. K. Pak, Neutron-proton mass difference in the Skyrme model, Phys. Lett. **159B**, 357 (1985); **162B**, 405(E) (1985).
[22] N. G. Deshpande, D. A. Dicus, K. Johnson, and V. L. Teplitz, Hadron electromagnetic mass differences, Phys. Rev. D **15**, 1885 (1977).
[23] A. Ebrahim and M. Savci, Electromagnetic neutron proton mass difference in the Skyrme model, Phys. Lett. B **189**, 343 (1987).
[24] L. N. Epele, H. Fanchiotti, C. A. Garcia Canal, and R. Mendez Galain, $\rho - \omega$ mixing and the $n - p$ mass difference, Phys. Rev. D **39**, 1473 (1989).
[25] P. Jain, R. Johnson, N. W. Park, J. Schechter, and H. Weigel, The neutron-proton mass splitting puzzle in Skyrme and chiral quark models, Phys. Rev. D **40**, 855 (1989).
[26] B. Y. Park and M. Rho, Neutron proton mass difference in the chiral hyperbag, Phys. Lett. B **220**, 7 (1989).
[27] J. M. Speight, A simple mass-splitting mechanism in the Skyrme model, Phys. Lett. B **781**, 455 (2018).
[28] E. Witten, Anti-de Sitter space and holography, Adv. Theor. Math. Phys. **2**, 253 (1998).
[29] T. Sakai and S. Sugimoto, Low energy hadron physics in holographic QCD, Prog. Theor. Phys. **113**, 843 (2005).
[30] T. Sakai and S. Sugimoto, More on a holographic dual of QCD, Prog. Theor. Phys. **114**, 1083 (2005).
[31] F. Bigazzi and P. Niro, Neutron-proton mass difference from gauge/gravity duality, Phys. Rev. D **98**, 046004 (2018).
[32] G.-W. Wu, M.-L. Yan, and K.-F. Liu, Flavor symmetry and mass splitting formulae for sub SU(3) skyrmion in SU(N), Phys. Rev. D **43**, 185 (1991).

[33] V. B. Kopeliovich, Semiclassical quantization of SU(3) skyrmions, J. Exp. Theor. Phys. **85**, 1060 (1997).
[34] G. H. Derrick, Comments on nonlinear wave equations as models for elementary particles, J. Math. Phys. (N.Y.) **5**, 1252 (1964).
[35] S. Bolognesi and W. Zakrzewski, Baby Skyrme model, near-BPS approximations and supersymmetric extensions, Phys. Rev. D **91**, 045034 (2015).
[36] S. B. Gudnason and J. M. Speight, Realistic classical binding energies in the ω-Skyrme model, J. High Energy Phys. 07 (2020) 184.
[37] D. Foster and N. S. Manton, Scattering of nucleons in the classical Skyrme model, Nucl. Phys. **B899**, 513 (2015).
[38] H. Hata, T. Sakai, S. Sugimoto, and S. Yamato, Baryons from instantons in holographic QCD, Prog. Theor. Phys. **117**, 1157 (2007).
[39] K. Hashimoto, T. Sakai, and S. Sugimoto, Holographic baryons: Static properties and form factors from gauge/string duality, Prog. Theor. Phys. **120**, 1093 (2008).
[40] O. Aharony and D. Kutasov, Holographic duals of long open strings, Phys. Rev. D **78**, 026005 (2008).
[41] D. K. Hong, M. Rho, H.-U. Yee, and P. Yi, Chiral dynamics of baryons from string theory, Phys. Rev. D **76**, 061901 (2007).
[42] S. Bolognesi and P. Sutcliffe, The Sakai-Sugimoto soliton, J. High Energy Phys. 01 (2014) 078.
[43] K. Hashimoto, T. Hirayama, and D. K. Hong, Quark mass dependence of hadron spectrum in holographic QCD, Phys. Rev. D **81**, 045016 (2010).
[44] K. Hashimoto, N. Iizuka, T. Ishii, and D. Kadoh, Three-flavor quark mass dependence of baryon spectra in holographic QCD, Phys. Lett. B **691**, 65 (2010).
[45] G. R. Filewood, Delta baryons in the separation geometry model, arXiv:hep-ph/0212328.
[46] P. A. Zyla *et al.* (Particle Data Group), Review of particle physics, Prog. Theor. Exp. Phys. **2020**, 083C01 (2020).
[47] E. Pedroni, A study of charge independence and symmetry from π^+ and π^- total cross-sections on hydrogen and deuterium near the 3,3 resonance, Nucl. Phys. **A300**, 321 (1978).
[48] V. V. Abaev and S. P. Kruglov, Phase shift analysis of πp scattering in the energy region from 160-MeV to 600-MeV, Z. Phys. A **352**, 85 (1995).
[49] A. Bernicha, G. Lopez Castro, and J. Pestieau, Pion-proton scattering and isospin breaking in the $\Delta^0 - \Delta^{++}$ system, Nucl. Phys. **A597**, 623 (1996).
[50] A. B. Gridnev, I. Horn, W. J. Briscoe, and I. I. Strakovsky, The K-matrix approach to the Δ-resonance mass splitting and isospin violation in low-energy πN scattering, Phys. At. Nucl. **69**, 1542 (2006).